Universidade de Aveiro Departamento de Química
2009

Ana Rute Marques Ferreira

MODELLING THE CARBON DIOXIDE SOLUBILITY WITH CPA EOS

MODELAÇÃO DA SOLUBILIDADE DO DIÓXIDO DE CARBONO COM A EQUAÇÃO DE ESTADO CUBIC PLUS ASSOCIATION

Universidade de Aveiro Departamento de Química
2009

Ana Rute Marques Ferreira

MODELLING THE CARBON DIOXIDE SOLUBILITY WITH CPA EOS

MODELAÇÃO DA SOLUBILIDADE DO DIÓXIDO DE CARBONO COM A EQUAÇÃO DE ESTADO CUBIC PLUS ASSOCIATION

Dissertação apresentada à Universidade de Aveiro para cumprimento dos requisitos necessários à obtenção do grau de Mestre em Engenharia Química, realizada sob a orientação científica do Dr. João Araújo Pereira Coutinho, Professor Associado com Agregação do Departamento de Química da Universidade de Aveiro.

Dedico este trabalho aos meus queridos pais e à minha manita.
Sem o apoio e o esforço deles, terminar esta tese teria sido muito mais difícil.
Obrigado por tudo!

o júri

presidente

Professora Doutora Maria Inês Purcell de Portugal Branco
Professora auxiliar do Departamento de Química da Universidade de Aveiro

Professor Doutor João Manuel da Costa e Araújo Pereira Coutinho
Professor associado com agregação do Departamento de Química da Universidade de Aveiro

Doutor António José Queimada
Investigador auxiliar da Faculdade de Engenharia da Universidade do Porto

agradecimentos

Tenho de começar por agradecer ao meu Orientador e Professor João Coutinho, pelo convite e pela oportunidade de poder trabalhar com estes novos solventes que tanto me fascinam, além de todo o incentivo e apoio que me foi dando ao longo do trabalho desenvolvido ("Só tu e mais umas duas ou três pessoas no mundo é que estão a fazer isto!").

Não me posso esquecer de todos os membros do PATh: Catarina, Mi, Ritinha, Claúdia, M. Jorge, Sónia, Juca, Mara, Ana, Samuel, Fatinha, Marise, Rui, Luciana, Bern, Liliana, Mayra, Kalpesh, mas principalmente da Mariana e do Pedro, foram quem mais e directamente me ajudaram:

Obrigado Marianita! És uma expert em CPA! Sem ti, não tinha ido muito longe! Não só pela imensa ajuda, como também por não me deixares desanimar quando os resultados não eram nada como nós gostávamos que fossem! És uma das melhores pessoas que já tive oportunidade de conhecer!

Obrigado Pedro! Por toda a tua paciência e vontade de ensinar! Foste fundamental na parte experimental deste trabalho! Davas um bom professor, sabias Chefinho?!

São um óptimo, divertido e inteligentíssimo grupo de investigação! Foi uma honra passar convosco este último ano! Muito obrigado a todos!

Obrigado Sofia, Clarinha, André, Vítor, João Tiago, Beto, Andreia, Nuno Dineia, Daniela, Dárcio, Alicia, Caroline, Ana Sofia e Sílvio! São amigos como poucos se podem gabar de ter! Espero nunca vos perder!

Obrigado meu Joel! Sem dúvida alguma, foste e és a minha muleta! Desculpa-me todos os maus momentos que esta tese te proporcionou e obrigado por partilhares o meu entusiasmo e os meus pequenos sucessos de modelação! Ajudaste-me muito mais do que imaginas!

E nem todos os obrigados do mundo eram capazes de quantificar a gratidão que sinto pelos meus pais! Sem eles, tudo era impossível! Obrigado por me amarem, apoiarem, incentivarem, aturarem, sustentarem e permanecerem sempre a meu lado! Espero não vos desiludir! Amo-vos muito!

Tu Maninha linda! És especial! És a última a quem agradeço, mas és quem está em primeiro lugar no meu coração! Obrigada por toda a loiça que lavaste e que não foi nada pouca! Desculpa por todo o meu mau humor e por tantas ser descarregado em ti! Espero que um dia consiga compensar-te! Obrigado por tudo! Gosto muito de ti!

Obrigado do fundo do coração!
Estou aqui, sempre que precisem!

palavras-chave

Dióxido de carbono, técnicas de captura de dióxido de carbono, líquidos iónicos,1-alquil-3-metilimidazólio bis(trifluorometilsulfonil)imida, equilíbrio líquido-vapor, equação de estado CPA, medições a altas pressões, dissulfureto de carbono, tetraclorometano.

resumo

As emissões de dióxido de carbono têm hoje uma grande importância na indústria de engenharia química, pelo que a sua captura e armazenamento são uma importante área de investigação. Os líquidos iónicos têm sido estudados como solventes (“green solvents”) para a separação de gases e captura de dióxido de carbono.

Os líquidos iónicos são uma nova classe de solventes orgânicos, que devido aos seus catiões orgânicos assimétricos e aos aniões inorgânicos, não podem constituir uma estrutura cristalina, permanecendo assim no estado líquido à temperatura ambiente ou temperaturas próximas desta.

Estes compostos apresentam uma vasta gama de propriedades interessantes, tais como a alta estabilidade térmica; o estado líquido numa grande amplitude térmica; a boa solvatação, tanto para compostos polares como não polares; e uma das mais interessantes, colocando-os como uma alternativa viável para substituir os solventes orgânicos voláteis, a sua pressão de vapor desprezável. Outra grande vantagem destes solventes "neotéricos" é a possibilidade de modelar as suas propriedades, através da infinita combinação de catiões e aniões, permitindo desenhar os líquidos iónicos de acordo com os objectivos específicos de uma operação particular melhorando o seu desempenho.

Já foram aplicadas várias equações de estado para descrever a solubilidade do dióxido de carbono nos líquidos iónicos (equilíbrio líquido-vapor), tais como a PC-SAFT, soft-SAFT, Peng-Robinson, Krichevsky-Kasarnovsky, entre outras equações de estado.

Neste trabalho, dados experimentais para o equilíbrio líquido-vapor do sistema de dióxido de carbono + 1-alquil-3-metilimidazólio bis(trifluorometilsulfonil)imida foram modelados pela primeira vez com a equação do estado Cubic Plus Association (CPA EoS), em que os parâmetros da equação são obtidos através do ajuste de dados experimentais de pressão de vapor e densidade. Com o objectivo de estudar a solubilidade do dióxido de carbono noutros compostos, foram também medidos os equilíbrios líquido-vapor dos sistemas dióxido de carbono + dissulfureto de carbono e dióxido de carbono + tetraclorometano, numa célula de alta pressão, e os dados experimentais obtidos foram igualmente modelados com a CPA EoS.

A equação de estado CPA já demonstrou ser uma ferramenta termodinamicamente flexível tendo descrito correctamente o equilíbrio líquido-vapor de misturas contendo componentes associativos e não associativos distribuídos por diferentes fases fluidas.

Mostra-se que este modelo permite uma boa descrição dos dados experimentais disponíveis.

keywords

Carbon dioxide, CO_2 capture tecniques, ionic liquids, 1-alkyl-3-methylimidazolium bis(trifluoromethylsulfonyl)imide, phase behavior, CPA EoS, high pressure experimental, carbon disulphide, carbon tetrachloride.

abstract

Carbon dioxide emissions have today a great importance in the chemical engineering industry, so its capture and storage are an important field of research. Ionic liquids have been studied as green solvents in gases separation and for carbon dioxide capture.

Ionic liquids are a new class of organic solvents that due to their asymmetric organic cations and organic or inorganic anions cannot form an ordered crystal and therefore remain liquid at or near room temperature.

These compounds present a wide range of interesting properties, such as high thermal stability, large liquid temperature range, good solvation both for polar and non polar compounds, and one of the most interesting, putting them as a viable and ambient friendly alternative to replace the volatile organic solvents, is their negligible vapor pressure. Other major advantage of these "neoteric" solvents is the possibility of fine tune their properties through the endless combination of cations and anions. This designer characteristic allows one to build task-specific ionic liquids that have an enhanced performance for specific operations.

Several equations of state have been applied to describe the carbon dioxide solubility in ionic liquids (vapor-liquid equilibrium) such PC-SAFT, soft-SAFT, Peng-Robinson EoS, Krichevsky–Kasarnovsky EoS, among others.

In this work, the experimental vapour-liquid equilibrium data of the systems carbon dioxide + 1-alkyl-3-methylimidazolium bis(trifluoromethylsulfonyl) imide ionic liquids were modelled for the first time with the Cubic plus Association Equation of State (CPA EoS) with the EOS parameters fitted to vapor pressure and densities of the ionic liquids. In addition, it was used a high pressure cell to measure the vapour-liquid equilibrium of the binary systems carbon dioxide + carbon disulphide and carbon dioxide + carbon tetrachloride and the experimental data obtained were also modelled with the CPA EoS.

The CPA EoS had already demonstrated to be a flexible thermodynamic tool for correctly modelling the phase equilibrium of mixtures containing both associative and non-associative components distributed by different fluid phases.

It is shown that this model allows for a very good description of the experimental data available.

CONTENTS

LIST OF TABLES

LIST OF FIGURES

NOMENCLATURE

List of symbols

a	energy parameter in the physical term
a_0	parameter in the energy term (a), Pa m^6 mol^{-2}
a_{ij}	cross-interaction energy parameter between molecules *i* and *j*
A_i	site A in molecule i
b	co-volume, m^3 mol^{-1}
c_1	parameter in the energy term, dimensionless
g	simplified radial distribution function
H	Henry's law constant, bar
k	binary interaction coefficient
n	mole number
N	mixture reference component
NP	number of points
P	vapour pressure, Pa
R	gas constant, Pa m^3 mol^{-1} K^{-1}
S	solubility
T	temperature, K
x	mole fraction
X_{A_i}	mole fraction of component i not bonded at site A
w	acentric factor
Z	compressibility factor

Greek letters

β	association volume
ρ	mole density, mol m^{-3}
σ	vapour
Δ	association strength
ε	association energy, J mol^{-1}
η	reduced liquid density

Subscripts

c	critical
i, j	pure component indexes
$liq.$	liquid
r	reduced

Superscripts

$assoc.$	association
$phys.$	physical

Abbreviations

AAD	average absolute deviation
COSMO-RS	conductor-like screening model for real solvents
CPA	cubic-plus-association equation of state
CR	combining rule
DEA	Diethanolamine
DIPA	Diisopropanolamine
ECR	Elliott combining rule
EoS	equation of state
GC-EoS	group contribution equation of state
Ils	ionic liquids
LD	length dependence
MDEA	N-Methyldiethanolamine
MEA	Monoethanolamine
OF	objective function
PC-SAFT	perturbed-chain statistical associating fluid theory
PR	Peng-Robinson equation
RK-EoS	Redlich-Kwong equation
SAFT	statistical associating fluid theory
SRK	Soave-Redlich-Kwong equation
SWCF	square well chain fluid equation
tPC-SAFT	truncated perturbed chain-polar statistical associating fluid theory
V	Values
VLE	vapour-liquid equilibrium
VOCs	volatile organic compounds

1. INTRODUCTION

The Earth's climate is largely a result of the physical and chemical properties of the atmosphere [1]. With the coming of Industrial era about 150 years ago, fossil fuel burning and forests clearing increased the atmospheric carbon dioxide levels to their present levels and as a result the atmospheric chemistry has drastically changed with dire consequences to the Earth's climate [1, 2].

To mitigate anthropogenic carbon dioxide emissions and climate changes, it is critical to develop new and more efficient technology to prevent carbon dioxide emissions or remove it from atmosphere altogether. Studies are being done in this area, such as the development of new industrial processes and new solvents and materials for CO_2 capture and storage [3-5].

Ionic liquids are one of the new classes of neoteric solvents in study, not only for CO_2 capture but also for many other applications in chemical process [6-9]. They are composed by organic cations and organic or inorganic anions and their properties can be tuned by changing the ions according to the desired properties. Their principal characteristics are the negligible vapour pressure, which made them a probable substitute for the organic volatile solvents, high thermal stability and being liquid in a broad range of temperatures.

This work addresses the study of the CO_2 solubility in ionic liquids and other solvents such as CS_2 and CCl_4.

1.1 Anthropogenic Carbon Dioxide

1.1.1 Carbon dioxide sources and effects

Anthropogenic carbon dioxide, after water vapour, is one of the gases responsible for the runaway greenhouse effect observed. Greenhouse effects is a physical effect of Earth's atmosphere [10] that consists on the trapping of the outgoing radiation by atmospheric gases, being water vapour and carbon dioxide the main contributors, in addition to others such methane, nitrous oxide, chlorofluorocarbons, etc., due to their great absorption capacity [11, 12]. These greenhouse gases are the responsible for the increase in the global temperature [10, 11].

Greenhouse gases concentrations have been increasing due to human activity in the atmosphere (see Figure 1), in particular carbon dioxide that increased approximately 33% during the last century [1], results in an intensification of the anthropogenic greenhouse effects when compared to the natural greenhouse effect, trapping more radiation (heat) which is believed to be one of the major causes of climate change [1, 10, 12, 13]. This temperature increase is responsible for the glaciers melting, sea level rising and consequent problems [4].

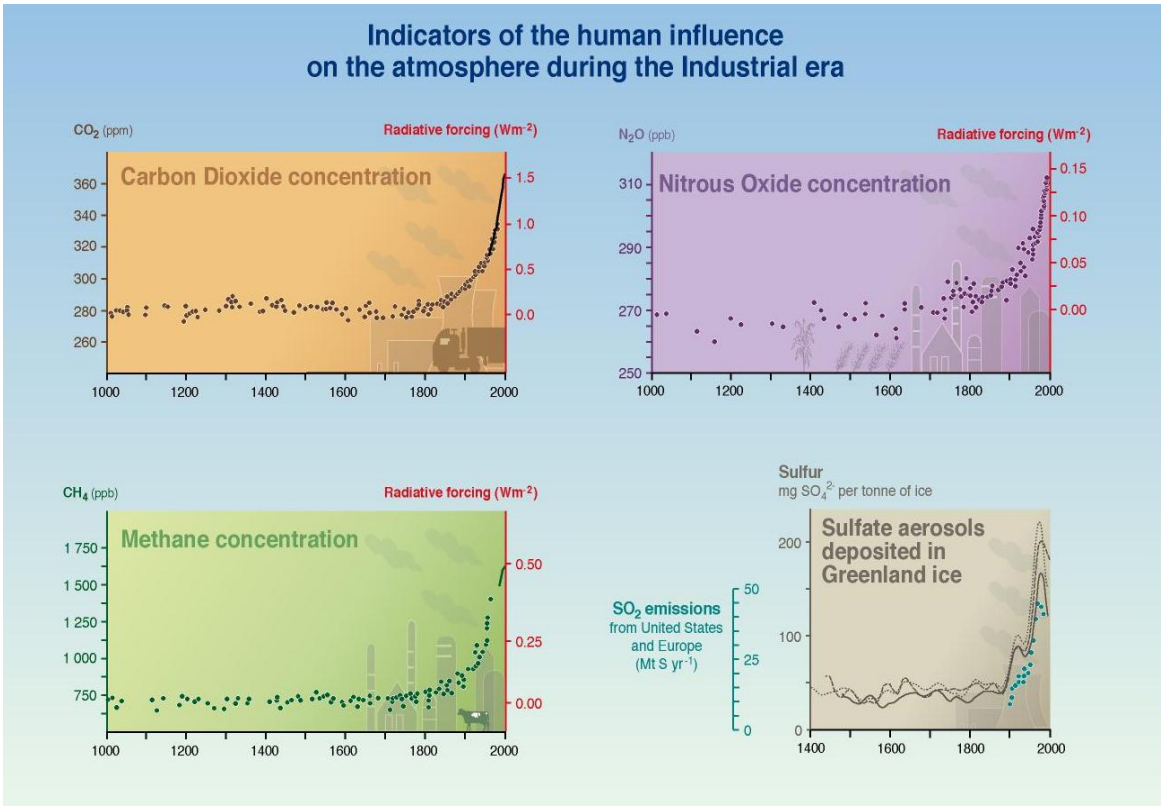

Figure 1 Indicators of human influence on the atmosphere during Industrial era [14].

But there are other ambient problems due to the atmospheric carbon dioxide concentration besides greenhouse effect and its consequences. The ocean is the largest natural receptacle for carbon dioxide, that dissolved, generates carbonate and bicarbonate ions. The increase of these ions increases ocean acidity, with unknown consequences to marine life [4].

The largest point source of anthropogenic carbon dioxide emissions, being responsible for more than 80% of the emissions [15], is the combustion of fossil fuels (oil, coal and natural gas) used in power plants, transportation, industrial facilities and uses such as in homes and commercial buildings (energy-related). There are yet other

sources that do not include fossil fuel combustion reaction but produce CO_2 as a by-product such as the cement industry, petroleum products in feedstock and end-uses, chemical and metals production [16].

With the aim to reduce CO_2 emissions many technologies, approaches, materials, solvents and molecules have been investigated and developed such as [3-5, 17]:

- Improve vehicles, appliances, and industrial process efficiencies to reduce fossil fuel consumption [4];
- Use alternative energy sources, such as wind, hydro, solar, nuclear, which are carbon dioxide emissions free [4];
- Carbon dioxide capture and storage into a geologic formation (consists in three steps: capture, transport and storage of carbon dioxide), ocean (which has been abandoned due to the environmental impact) or terrestrial ecosystems (through natural processes, such as the growth of plants and microorganisms) [4].

1.1.2 Carbon dioxide capture technologies

Carbon dioxide can be captured from power plants, industrial processes, or other sources, and there are three technological pathways to do it: post-combustion capture, pre-combustion capture, and oxy-combustion [2-5, 17-20], which rely on gas separation technologies with solvent/sorbents, membranes and cryogenic distillation.

In general, carbon dioxide capture technologies can provide a reduction of about 95% of carbon dioxide emissions [12].

- Post-combustion capture

This approach consists in removing carbon dioxide after fossils fuel combustion (Figure 2). Due to the low concentration, about 3-15% of the hot flue gas, the thermodynamic driving force for carbon dioxide capture is low, which requires higher performance or higher circulation volume of the solvents [21].

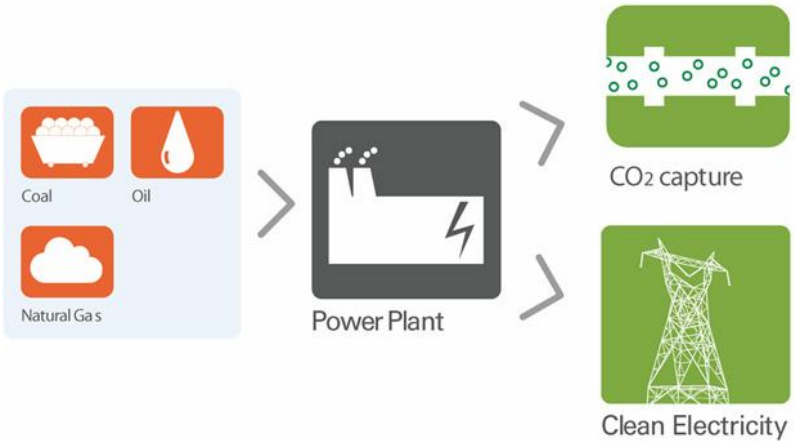

Figure 2 Post-combustion capture process diagram [21].

- Pre-combustion capture

In this approach, carbon dioxide is captured before fuel burning. Reduction in size and costs of carbon dioxide capture facilities can be achieved, if the concentration and pressure of CO_2 can be increased [3, 19].

One method for this approach is the gasification process (Figure 3), which converts the fuel in carbon monoxide and hydrogen - “syngas”. Then carbon monoxide reacts with steam producing carbon dioxide (at high concentration (35-45%) and high pressure) and additional hydrogen. After this second reaction, the carbon dioxide produced can be captured by diverse separation technologies and the resulting hydrogen can generate CO_2-free electricity, producing only heat and water vapour of its burning [3-5, 17, 19, 21, 22].

Despite being more complex and consequently more expensive than processes involved in post-combustion, due to the high concentration of carbon dioxide produced and its high partial pressure, this process can be cost-effectively used to make large amounts of clean hydrogen for the power industry as well as in refineries and other chemical industries [3, 19, 21].

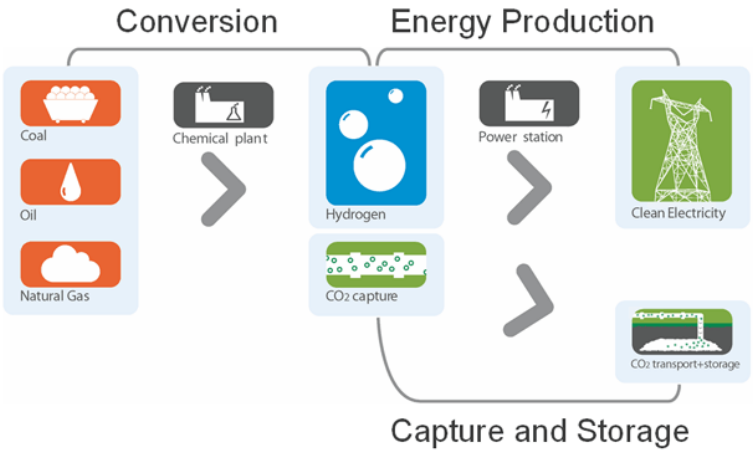

Figure 3 Pre-combustion capture process diagram [21].

- Oxy-combustion

This is an alternative for CO_2 capture from flue gas and consists in burn the fossil fuel with nearly pure oxygen (greater than 95%), instead of air, mixed with flue gas. This results in an exhaust gas consisting predominantly of concentrated CO_2 and water vapour. The CO_2 (typically greater than 80% by volume) is then easily captured after remove water vapour by cooling and compressing the gas stream [3, 21, 22].

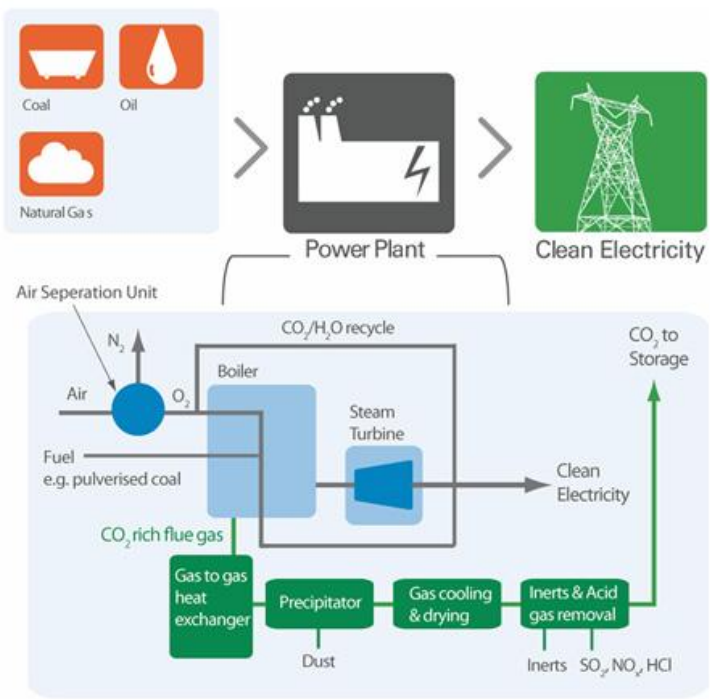

Figure 4 Oxy-combustion process diagram [21].

1.1.2.1 Currently available carbon dioxide capture processes:

► Chemical solvents:

- Amines solutions:

Amines react with carbon dioxide to form a water soluble compound:

$$R-NH_2 + CO_2 + H_2O \rightarrow R-NH_3^+ + HCO_3^- \quad (1)$$

The conventional alkanolamines used in aqueous organic medium or in combination with aqueous potassium carbonate are [23]:

- Monoethanolamine (MEA)
- Diethanolamine (DEA)
- Diisopropanolamine (DIPA)
- N-Methyldiethanolamine (MDEA)

But these solvents make post-combustion an expensive stage due to intensive energy consumption, cost increases and corrosion problems caused by the high energy consumption for regenerating amine solutions, parallel loss of the volatile amines, the uptake of water into the gas stream and low pressure of the gas stream.

To improve the system performance many modifications can be implemented such as amine modifications, packing towers modifications to reduce pressure drop and increase contacting, increase heat integration to reduce energy requirements, use of additives to reduce corrosion and allow higher amine concentration and improved regenerating procedures [3, 4, 23] .

- Potassium carbonate:

It consists in converting carbonate to bicarbonate in the presence of carbon dioxide. When heated the reaction reverts for the carbonate releasing carbon dioxide:

$$K_2CO_3 + CO_2 + H_2O \leftrightarrow 2KHCO_3 \quad (2)$$

This process and structure packing improvements present some improvements compared to amine solutions due to the lower energy requirements for regeneration.

► Physical solvents:

The performance of physical solvents depends on the solvent used, the partial pressure of carbon dioxide and operating temperature. Therefore higher loadings are achieved with higher partial pressures and lower temperatures.

The most common physical solvents used are Selexol (mixture of dimethyl ethers of polyethylene glycol), Rectisol (chilled methanol) and propylene carbonate [4, 17, 19].

► Emerging technologies:

New technologies are being investigated to improve efficiency and costs over carbon dioxide capture, being some of them reported below. In Figure 5 it can be seen the potential cost reduction benefits once innovative carbon dioxide capture technologies are commercialized.

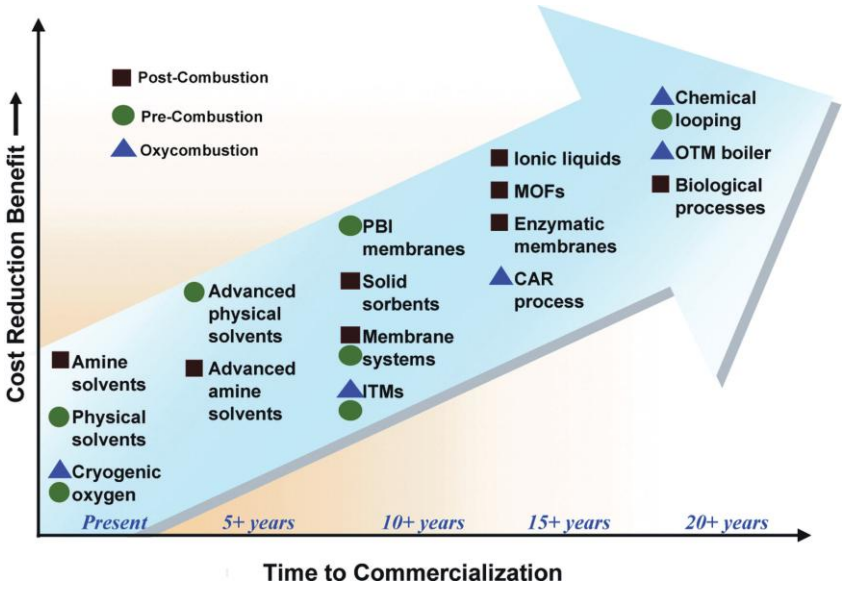

Figure 5 Cost reduction benefits of innovative CO_2 capture technologies versus time to commercialization [3, 4].

- Aqueous ammonia

Aqueous ammonia scrubbing principles are similar to those for amine systems. Ammonia reacts with CO_2 forming ammonium carbonate which can react with additional CO_2 to form ammonium bicarbonate:

$$2NH_3 + CO_2 + H_2O \rightarrow (NH_4)_2CO_3 \quad (3)$$

$$(NH_4)_2CO_3 + CO_2 + H_2O \rightarrow 2NH_4HCO \quad (4)$$

This process has some advantages such as the lower heat of reaction which results in energy savings, lower energy requirements at lower pressures, low cost, potential for high carbon dioxide capacity, lack of degradation and higher tolerance for oxygen in the flue gas [3, 4].

- Membranes

In post-combustion capture, since the partial pressure of CO_2 in a typical flue gas is considerably low, vacuum is required on the permeate side or a sweep gas must be used, requiring a further separation. Because of the higher partial pressure of CO_2 in the raw syngas, the use of membranes with pre-combustion capture is more promising [3, 4, 19].

- Regenerable solid sorbents

Solids can act as physical sorbents or form a chemical compound at one set of operating conditions and be regenerated at another set of conditions, releasing the adsorbed CO_2 and regenerating the original compound. One example of these compounds is sodium carbonate [3, 4].

Handling difficulties are inherent to solids, where moving (or fluidized) beds for the solids or fixed beds with periodic gas flow switching can be used. Due to the large volume of flue gas from a typical coal-fired power plant, large equipments will be necessary [3, 4].

- Metal organic frameworks (MOFs)

MOFs are a new group of hybrid material with possible high CO_2 capacity and low energy requirements for regeneration. They are built from metal ions with well-defined coordination geometry and organic bridging ligands and are extended structures with carefully sized cavities that can adsorb CO_2 [3, 4].

- Enzyme-based systems

Carbozyme is developing enzyme-based systems which utilizes carbonic anhydrase (CA) in a hollow fiber contained liquid membrane having, in laboratory scale, the potential to capture 90% of CO_2 followed by regeneration at ambient temperature. These systems can capture and release carbon dioxide by mimicking of the mammalian respiratory system [3, 19].

1.2 Ionic Liquids

Ionic liquids are a new class of neoteric organic solvents that can be applied to a large number of process and chemical reactions. Due to their unique attractive properties it is expected that their use may have a strong impact in chemical engineering in the near future [24]. Therefore many studies have been carried to develop and increase the available information and knowledge about these new solvents in recent years, as can been seen in Figure 6.

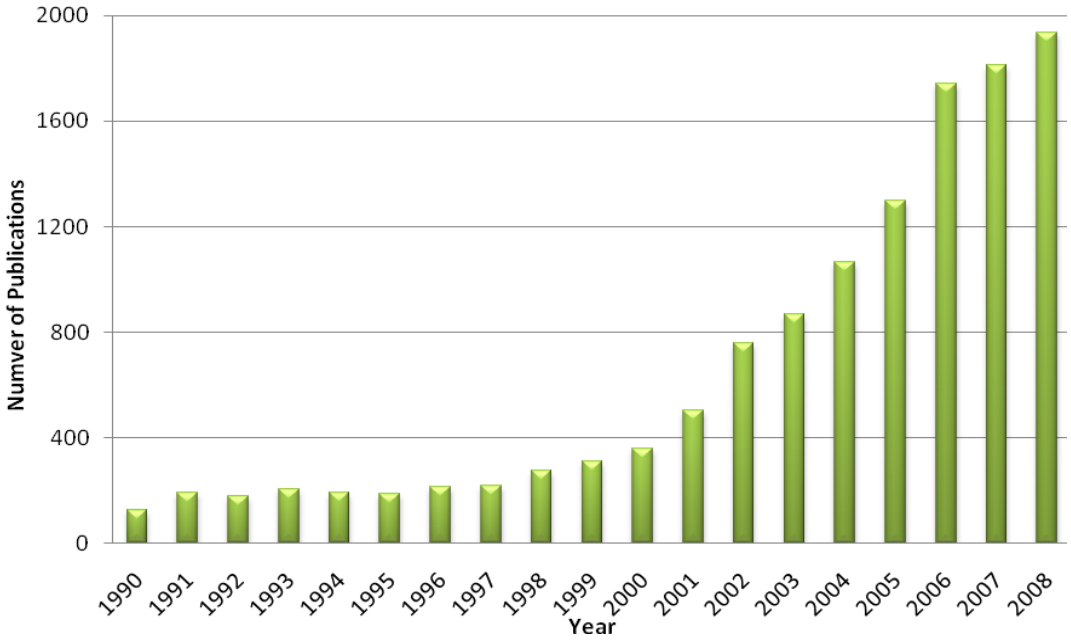

Figure 6 Number of publications about ionic liquids since 1990 to 2008 (results from Web of Science, May of 2009).

Ionic liquids are molten salts generally composed by a large asymmetric organic cation and an organic or inorganic anion in equal number by which they are electrically neutral [25].

The cations families most studied are the imidazolium, pyridinium, pyrrolidinium and phosphonium based while the anions can be bis(trifluoromethylsulfonyl)imide, tetrafluoroborate, hexafluorophosphate, halogenates, among many others. Some of these ions are illustrated in Table 1.

Table 1 Names, abbreviations and structures of the most common cations and anions.

Name	Abbreviation	Structure
Most common cations		
1,3-dimethylimidazolium; R=CH_3	$[dmim]^+$	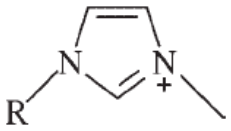
1-ethyl-3-methylimidazolium; R=C_2H_5	$[C_2mim]^+$ or $[emim]^+$	
1-butyl-3-methylimidazolium; R=C_4H_9	$[C_4mim]^+$ or $[bmim]^+$	
1-pentyl-3-methylimidazolium; R=C_5H_{11}	$[C_5mim]^+$ or $[pmim]^+$	
1-hexyl-3-methylimidazolium; R=C_6H_{13}	$[C_6mim]^+$ or $[hmim]^+$	
1-N-butyl-3-methylpyridinium; R=C_4H_9	$[bmpy]^+$	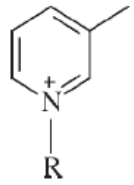
1-N-hexyl-3-methylpyridinium; R=C_5H_{11}	$[hmpy]^+$	
1-butyl-1-methylpyrrolidinium	$[bmpyrr]^+$	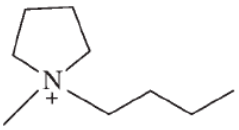
Tetrabutylphosphonium	$[P(C_4)_4]^+$	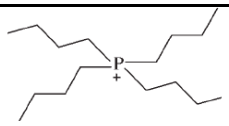
Most common anions		
Tetrafluoroborate	$[BF_4]^-$	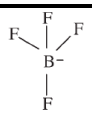
Hexafluorophosphate	$[PF_6]^-$	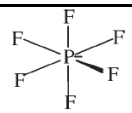
Bis(trifluoromethylsulfonyl)imide	$[NTf_2]^-$	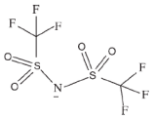
1,1,2,3,3,3-Hexafluoropanesulfonate	$[HFPS]^-$	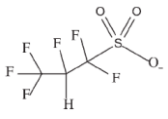
Methyl sulfate	$[MeSO_4]^-$	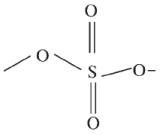

By choosing specific ions and/or functional groups, ionic liquid properties can be tuned and so the ionic liquids can be designed for a particular application.

In spite of this diversity, ionic liquids share some common properties such as negligible vapour pressures, which results in very low volatility and reduce fire hazards, high thermal stability, low melting points, large liquid range covering room or near room temperatures, adjustable solvation behaviour with good solvating capacity for both organic and inorganic compounds.

These salts are liquid in a wide range of temperatures due to their negative Gibbs free energy of fusion, small lattice enthalpy and large entropy changes which are a result from the large asymmetric cations, conformational flexibility of the ions and weak coulombic forces, which cannot form a crystalline structure like common salts [6, 25-27].

There are many possible ionic liquid applications in the chemical industry. Ionic liquids can be used as solvents in chemical reactions and process separation, such as in catalytic reactions, cleaning and purifications operations, gas separations, liquids separations and as gas storage, electrolyte in fuel cells, lubricants and heat transfer fluids, being the most interesting research areas the replacement of volatile organic compounds and gas separation [7-9, 26, 28-30].

Ionic liquids are considered a possible replacement for conventional volatile organic compounds (VOCs) used in the chemical industry because of their negligible vapour pressure, having a lower impact on air pollution and environmental benefits [26, 28, 29, 31, 32]. Yet they are miscible with water [33, 34] which can be a path to enter on the environment. For some ionic liquids their toxicity and impact on aquatic ecosystems has been studied. The imidazolium and pyridinium based Ils have a toxicity inferior to most organic solvents that seems to increase with the cation alkyl chain length while the anion influence is smaller than that of the cation. Their toxicity can also be controlled and minimized tuning ionic liquid properties by an adequate choice of the ions that compose the ionic liquid [33].

The interest in ionic liquids for gas separations results also from their non-volatility which cannot contaminate gas streams, their high stability which made their use possible at higher temperatures making possible their use in conventional absorbers and strippers [26] or supported liquids membranes, reducing the amount of solvent necessary because the reduced loss of solvent and not-degradation of the membrane with time [26, 35].

The knowledge of gas solubility in ionic liquid, among other mixture properties, is essential for ionic liquids application in chemical processes and their development, being carbon dioxide solubility one of the most investigated aiming at their use in CO_2 capture processes.

1.3 Carbon Dioxide solubility in Ionic Liquids

Carbon dioxide solubility in ionic liquids has not been studied only aiming at carbon dioxide capture and gas separation, but also because supercritical carbon dioxide can be used to extract compounds from ionic liquids and to separate ionic liquids from organic liquid mixtures promoting phase separation without contamination of the ionic liquid [7, 26, 36].

Some researchers have demonstrated that the carbon dioxide is one of the most soluble gases in ionic liquids, making ionic liquids capable of gas separation for natural gas and flue gas [26]. Carbon dioxide solubility in ionic liquids is affected by cations and/or anions change, degree of fluorination of the anion or the cation and other CO_2-philic groups [26, 36].

Solubility can be expressed by the Henry's constant, being solubility inversely correlated to the Henry's law constant ($P = H \times S$). Table 2 presents some Henry's law constants for carbon dioxide solubility in some ionic liquids. It allows the comparison of the carbon dioxide solubility in some ionic liquids and the influence of the ions and functional groups.

Table 2 Henry's law constants for carbon dioxide in several ionic liquids at 298K [26].

Compound	*H* (bar)
$[C_4mim][PF_6]$	53.4 ± 0.3
$[C_4mim][BF_4]$	59.0 ± 2.6
$[C_4mim][NTf_2]$	33.0 ± 0.3
$[C_6mim][NTf_2]$	31.6 ± 0.2
$[C_6mpy][NTf_2]$	32.8 ± 0.2
$[C_6H_4F_9mim][NTf_2]$	28.4 ± 0.1
$[C_8H_4F_{13}mim][NTf_2]$	27.3 ± 0.2

Cations changes do not have a considerable influence in carbon dioxide solubility being this mostly affected by the anions [7, 26]. Fixing the cation $[C_4mim]^+$ and comparing the anions $[NTf_2]^-$, $[BF_4]^-$ and $[PF_6]^-$, it can be observed that the solubility is drastically different for each anion, noting that it decreases from $[NTf_2]^-$ to $[PF_6]^-$ to $[BF_4]^-$ [26]. Fixing the anion $[NTf_2]^-$ and varying the cation, such $[C_6mim]^+$, $[C_6mpy]^+$ and $[N_{4111}]^+$, the solubility is similar for all ionic liquids. For some cations, such as choline, carbon dioxide solubility is lower, which can be explained by the stronger hydrogen bonding between the choline and $[NTf_2]^-$ making the anion less available to interact with the carbon dioxide [26]. These comparisons suggest that the interaction of carbon dioxide with the anion is higher than that with the cation.

Comparing imidazolium based ionic liquids, such $[C_nmim][NTf_2]$, $[C_nmim][BF_4]$ and $[C_nmim][PF_6]$ the increase in the cation alkyl chain length slightly increases the carbon dioxide solubility in the ionic liquids due to the highest free volume in the ionic liquid, but this effect is minor compared to that of the anion [26].

Addition of fluoroalkyl groups to the cation or anion seems to increase the carbon dioxide solubility, but this increase will occur only until the maximum CO_2-philicity is reached which correspond to an optimum number of fluorine atoms in the fluoroalkyl chain [36].

2. MODEL

Due to the very large number of possible ionic liquids, it is necessary to develop correlations and predictive models able to describe behaviours and properties based on experimental measurements of selected systems. Several models have already been applied to carbon dioxide and ionic liquid systems, such as tPC-SAFT [24, 37], soft-SAFT [32], COSMO-RS [38], SWCF-EoS [28, 39], RK-EoS [29, 40], GC-EoS [41] and Krichevsky–Kasarnovsky EoS [42] , but the Cubic Plus Association equation of state (CPA EoS) is being applied for the first time in this work as a model for ionic liquids systems.

The CPA EoS was proposed by Kontogeorgis and co-workers [43] and since 1995 has been developed and applied to diverse systems showing great results on the description of phase behaviour. The systems for which it already have been applied were composed by associating components and/or non associating components and the results were improved compared to others obtained with equations that only take into account one binary interaction parameter such as the PR EoS and the SRK EoS, among others [43].

2.1 Cubic plus Association Equation of State

The CPA EoS is composed by two terms: one is the physical term described by the Soave-Redlich-Kwong equation of state (SRK EoS), which takes into account the physical interactions between the components, and the other is related to the associating term and is described by the Wertheim's theory accounting for the specific site-site interactions due to hydrogen bonding and solvation effects [43].

In terms of the compressibility factor, the CPA EoS is expressed by the following equation [43]:

$$\begin{aligned} Z &= Z^{phys.} + Z^{assoc.} \\ &= \frac{1}{1-b\rho} - \frac{a\rho}{RT(1+b\rho)} \\ &\quad - \frac{1}{2}\left(1+\rho\frac{\partial \ln g}{\partial \rho}\right)\sum_i x_i \sum_{A_i}\left(1-X_{A_i}\right) \end{aligned} \tag{5}$$

where a is the energy parameter, b the co-volume, ρ the density of the liquid, g the simplified radial distribution function, x_i the mole fraction of the component i and X_{A_i} the mole fraction of pure component i not bonded at site A.

The energy parameter for pure components is given by a Soave-type temperature dependency:

$$a = a_0\left[1 + c_1\left(1 - \sqrt{T_r}\right)\right]^2, \tag{6}$$

where T_r is the reduced temperature ($T_r = T/T_c$, being T_c the critical temperature). The a_0 and c_1 constants are estimated by fitting experimental vapour pressure and liquid density data of the pure component.

X_{A_i} is the central point of the association term, is related to the association strength between site A on molecule i and site B on molecule j ($\Delta^{A_iB_j}$) and is calculated by solving the following set of equations:

$$X_{A_i} = \frac{1}{1 + \rho\sum_j x_j \sum_{B_j} X_{B_j}\Delta^{A_iB_j}}, \tag{7}$$

where B_j represents the summation over all sites and depends on the class of the association scheme.

The association strength $\Delta^{A_iB_j}$ is given by:

$$\Delta^{A_iB_j} = g(\rho)\left[\exp\left(\frac{\varepsilon^{A_iB_j}}{RT}\right) - 1\right] b_{ij}\beta^{A_iB_j}, \tag{8}$$

where $\varepsilon^{A_iB_j}$ is the association energy and $\beta^{A_iB_j}$ the association volume. When self-association occurs, the association strength $\Delta^{A_iB_j}$ becomes $\Delta^{A_iB_i}$:

$$\Delta^{A_iB_i} = g(\rho)\left[\exp\left(\frac{\varepsilon^{A_iB_i}}{RT}\right)-1\right]b_{ii}\beta^{A_iB_i}. \quad (9)$$

The simplified radial distribution function, $g(\rho)$, is expressed as:

$$g(\rho) = \frac{1}{1-1.9\eta}, \quad (10)$$

where η is the reduced liquid density given by $\eta = \frac{1}{4}b\rho$.

Therefore the CPA EoS has five pure compound parameters, three for non-associating compounds: a_0, c_1 and b and two for associating compounds: $\varepsilon^{A_iB_j}$ and $\beta^{A_iB_j}$. These pure compound parameters are obtained for each compound by fitting experimental vapour pressure and liquid density data.

The objective function used for the regressing of the pure compound parameters [44, 45] is:

$$OF = \sum_i^{NP}\left(\frac{P_i^{\exp.} - P_i^{calc.}}{P_i^{\exp.}}\right)^2 + \sum_i^{NP}\left(\frac{\rho_i^{\exp.} - \rho_i^{calc.}}{\rho_i^{\exp.}}\right)^2. \quad (11)$$

- *Mixtures*

When the CPA EoS is employed to mixtures, it is necessary to apply mixing and combining rules to the physical parameters. Those here applied are the van der Waals one-fluid mixing/combining rules:

$$a = \sum_i\sum_j x_i x_j a_{ij}, \qquad \text{where } a_{ij} = \sqrt{a_i a_j}\left(1-k_{ij}\right) \quad (12)$$

being k_{ij} the binary interaction parameter and

$$b = \sum_i x_i b_i. \quad (13)$$

The objective function used for the estimation of the binary interaction parameter is:

$$OF = \sum_{i}^{NP} \left(\frac{x_i^{\exp.} - x_i^{calc.}}{x_i^{\exp.}} \right)^2 \tag{14}$$

When the system is composed only by non-associating compounds, the CPA EoS reduces to the SKR EoS, being required only the three pure compound parameters of the physical contribution.

For binary mixtures with self-associating and non-associating compounds, the binary interaction parameter is the only adjustable parameter and combining rules are not needed for the association energy and volume [44].

For cross-associating compounds (association between different molecules), combining rules for the energy and volume of association are also required. From some investigations [43, 46, 47], different sets of combining rules have been proposed including for $\varepsilon^{A_iB_j}$, $\beta^{A_iB_j}$ and the association strength ($\Delta^{A_iB_j}$):

$$\varepsilon^{A_iB_j} = \frac{\varepsilon^{A_iB_i} + \varepsilon^{A_jB_j}}{2}\ ,\ \beta^{A_iB_j} = \frac{\beta^{A_iB_i} + \beta^{A_jB_j}}{2}, \tag{15}$$

which are referred as CR-1 set [43, 48, 49];

$$\varepsilon^{A_iB_j} = \frac{\varepsilon^{A_iB_i} + \varepsilon^{A_jB_j}}{2},\ \beta^{A_iB_j} = \sqrt{\beta^{A_iB_i}\beta^{A_jB_j}}\ , \tag{16}$$

which are referred as CR-2 set [48, 49];

$$\varepsilon^{A_iB_j} = \sqrt{\varepsilon^{A_iB_i}\varepsilon^{A_jB_j}}\ , \beta^{A_iB_j} = \sqrt{\beta^{A_iB_i}\beta^{A_jB_j}}\ , \tag{17}$$

which are referred as CR-3 set [48, 49];

$$\Delta^{A_iB_j} = \sqrt{\Delta^{A_iB_i}\Delta^{A_jB_j}}\ , \tag{18}$$

which is referred as CR-4 set (or Elliot rule, ECR) [43, 48, 49].

From these combining rules the most commonly used are the CR-2 set and the CR-4 sets [48].

- *Association scheme*

The association scheme is related to the number and type of association sites for the associating compounds. There are several schemes classified by Huang and Radosz [50], which can been seen in Table 3.

The 1A scheme is applied to acids and assumes that the acid groups work as a glue spot able to bond with a lone pair of electrons, a H atom or a site of the same type.

The schemes 2B or 3B are applied to alcohols and amines. The scheme 2B assumes that hydrogen bonding occurs between the hydroxyl hydrogen and one of the lone pairs of electrons from the oxygen atom of another alcohol molecule.

The scheme 4C is used for highly hydrogen bonded substances, as glycols and water, and assumes that hydrogen bonding occurs between the two hydrogen atoms and the two lone pairs of electrons in the oxygen of another molecule.

Table 3 Association schemes based on the terminology of Huang and Radosz [43, 50].

Species	Formula	Type
Acids	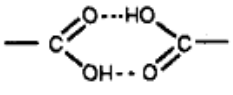	1A
Alcohols		3B
		2B
Glycols	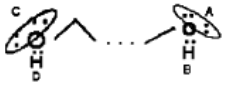	4C
Water	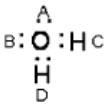	4C
	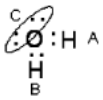	3B
	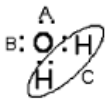	3B

2.2 Results and Discussion

Ionic liquids from the $[C_n mim][NTf_2]$ series were the ionic liquids selected for the study of the CPA EoS application and its performance on describing carbon dioxide solubility behaviour in ionic liquids.

2.2.1 Compilation and selection of available data

Before starting modelling, there are some experimental data required, such as vapour pressure and liquid density data and critical properties for the compounds in study.

Vapour pressure (P^{σ}) and liquid density ($\rho^{liq.}$) data for carbon dioxide were obtained from the DIPPR database [51], which are described by the following correlations (the constants are present in Table B 1 and Table B 2 (Appendix B)):

$$P^{\sigma} = \exp\left[A + \frac{B}{T} + C \times \ln T + D \times T^{E}\right], \tag{19}$$

$$\rho^{liq.} = \frac{A}{B^{\left[1+\left(1-\frac{T}{C}\right)^{D}\right]}}. \tag{20}$$

The usually reduced temperature range applied is from 0.45 to 0.85, which covers most of the liquid range, from close to the triple point to the critical point. However, due to the limited temperature range of the DIPPR database for carbon dioxide data, the reduced temperature range covered was from 0.71 to 0.90.

Carbon dioxide critical properties were also obtained from the DIPPR database [51] (Table A 1, Appendix A).

Being ionic liquids such new solvents, available data for some investigations is sometimes scarce, which is why it was necessary a review of the available or supplied vapour pressure, liquid density data and vapour-liquid equilibrium data (PTx) for the ionic liquids under study (Table 4).

Table 4 Ionic liquids studied and availability of data.

Compound	P^{σ}	$\rho^{liq.}$	PTx
$[C_2mim][NTf_2]$	✓	✓	✓
$[C_3mim][NTf_2]$	×	✓	×
$[C_4mim][NTf_2]$	✓	✓	✓
$[C_5mim][NTf_2]$	×	✓	✓
$[C_6mim][NTf_2]$	✓	✓	✓
$[C_7mim][NTf_2]$	×	✓	×
$[C_8mim][NTf_2]$	✓	✓	×

Liquid phase density data for ionic liquids were obtained from the literature [52-54] and vapour pressure data were obtained from a correlation (equation 21) provided by Prof. Luis Belchior Santos, from University of Porto developed based on data measured at his laboratory (constants in Table B 3, Appendix B).

$$\ln\left(\frac{P}{P^{\sigma}}\right) = A - \frac{B}{T}, \text{ with } P = 1Pa \tag{21}$$

The critical properties for the ionic liquids studied were obtained from Valderrama et al., estimated applying the modified Lydersen-Joback-Reid method there proposed [55, 56] (Table A 2, Appendix A).

2.2.2 Correlation of the CPA pure compound parameters

The estimation of the pure compounds parameters is a crucial step before applying the equation of state. It was carried out, as mentioned before, by simultaneous regression of vapour pressure and liquid density data for non-associating and associating compounds using the equation 11.

This was achieved using a FORTRAN routine based on a modified Marquardt algorithm for non-linear least squares, which was obtained from the Harwell subroutine library (http://hsl.rl.ac.uk/archive/cou.html). This routine allows constrained regression of the CPA parameters, so the user can set up the range of allowed values for each parameter, avoiding the regression of parameters with non-physical meaning.

The global average deviation (%AAD) for vapour pressure or liquid density is calculated by:

$$\%AAD = \frac{1}{NP}\sum_{i=1}^{NP} ABS\left[\frac{X_{\exp,i} - X_{calc,i}}{X_{\exp,i}}\right] \times 100, \tag{22}$$

where X can be vapour pressure or liquid density.

Carbon dioxide is considered as a non-associative compound therefore only three parameters of the physical part of the equation of state are required (Table 5).

Table 5 CPA pure compound parameters and modelling results for carbon dioxide.

Compound	a_0 (Pa m^6 mol^{-2})	c_1	$b \times 10^4$ (m^3 mol^{-1})	%AAD P^σ	%AAD $\rho^{liq.}$
CO_2	0.35	0.76	0.27	0.22	0.83

The study about the present ionic liquids was carried taking into account non-associative and associative interactions between the ionic liquids and the association scheme was also investigated.

In a first approach the ionic liquids are treated as non-associating compounds and therefore only the three physical parameters were estimated. These pure parameters are reported in Table 6.

Table 6 CPA pure compound parameters and modelling results for the $[C_n mim][NTf_2]$ series, considering non- association.

Compound	a_0 (Pa m^6 mol^{-2})	c_1	$b \times 10^4$ (m^3 mol^{-1})	%AAD P^σ	%AAD $\rho^{liq.}$
$[C_2mim][NTf_2]$	25.12	0.58	2.95	2.27	1.06
$[C_3mim][NTf_2]$	24.48	0.49	2.67	0.50	0.62
$[C_4mim][NTf_2]$	25.56	0.52	2.85	0.88	0.84
$[C_5mim][NTf_2]$	25.08	0.57	2.91	0.67	0.62
$[C_6mim][NTf_2]$	25.62	0.66	3.18	0.28	0.61
$[C_7mim][NTf_2]$	24.85	0.80	3.38	2.96	1.33
$[C_8mim][NTf_2]$	25.14	0.89	3.56	3.28	1.36
Global %AAD				1.55	0.92

Considering ionic liquids as associating compounds (self-associating compounds), the association schemes 1A, 2B and 4C were studied, and it became then necessary to estimate the five pure compound parameters.

The parameter values depend on the chosen association scheme. The parameters were determined for scheme 1A for all the ionic liquids in this study and schemes 2B and 4C for $[C_2mim][NTf_2]$, $[C_4mim][NTf_2]$, $[C_5mim][NTf_2]$ and $[C_6mim][NTf_2]$.

Tables 7, 8 and 9 report the respective parameters for each association scheme.

Table 7 CPA pure compound parameters and modelling results for the [$C_n$mim][NTf_2] series, considering scheme 1A.

Compound	a_0 (Pa m^6 mol^{-2})	c_1	$b\times10^4$ (m^3 mol^{-1})	$\varepsilon^{A_iB_i}\times10^{-4}$ (J mol^{-1})	$\beta^{A_iB_i}\times10^2$	%AAD P^σ	%AAD ρ^{liq}
[C_2mim][NTf_2]	10.95	0.92	2.86	8.93	6.35	0.49	0.77
[C_3mim][NTf_2]	13.97	0.66	2.63	7.33	4.91	0.19	0.54
[C_4mim][NTf_2]	14.72	0.68	2.80	7.45	3.40	0.63	0.72
[C_5mim][NTf_2]	16.08	0.69	2.87	6.62	2.77	0.21	0.55
[C_6mim][NTf_2]	16.68	0.75	3.14	7.04	0.98	0.32	0.55
[C_7mim][NTf_2]	18.02	0.74	3.35	8.02	0.06	2.10	1.39
[C_8mim][NTf_2]	18.83	0.83	3.51	7.51	0.08	2.37	1.23
Global %ADD						0.90	0.82

Table 8 CPA pure compound parameters and modelling results for the $[C_n mim][NTf_2]$ series, considering scheme 2B.

Compound	a_0 (Pa m^6 mol^{-2})	c_1	$b\times10^4$ (m^3 mol^{-1})	$\varepsilon^{A,B_i}\times10^{-4}$ (J mol^{-1})	$\beta^{A,B_i}\times10^2$	%AAD P^σ	%AAD ρ^{liq}
$[C_2mim][NTf_2]$	25.79	0.36	2.98	2.54	1.87	2.35	1.59
$[C_4mim][NTf_2]$	14.80	0.71	2.80	3.41	36.90	0.68	0.81
$[C_5mim][NTf_2]$	15.13	0.68	2.86	3.89	12.70	0.26	0.56
$[C_6mim][NTf_2]$	16.68	0.75	3.13	7.04	0.98	0.32	0.55
Global %ADD						0.90	0.88

Table 9 CPA pure compound parameters and modelling results for the $[C_n mim][NTf_2]$ series, considering scheme 4C.

Compound	a_0 (Pa m^6 mol^{-2})	c_1	$b\times10^4$ (m^3 mol^{-1})	$\varepsilon^{A,B_i}\times10^{-4}$ (J mol^{-1})	$\beta^{A,B_i}\times10^2$	%AAD P^σ	%AAD ρ^{liq}
$[C_2mim][NTf_2]$	7.63	0.35	3.41	4.70	1.49	0.30	0.73
$[C_4mim][NTf_2]$	5.59	0.28	2.61	4.79	1.78	0.06	0.59
$[C_5mim][NTf_2]$	5.31	0.63	2.71	4.58	2.08	0.38	0.44
$[C_6mim][NTf_2]$	5.11	0.76	2.94	4.83	1.25	0.20	0.43
Global %ADD						0.24	0.55

As can be seen from the previous tables, a good description of vapour pressure and liquid densities can be achieved with CPA for carbon dioxide and the various ionic liquids studied, being the global average deviation inferior to 1%, with a decrease in the deviation when association is considered. The parameters obtained are higher than the expected when compared to pure parameters for other compounds [43].

Figures 7 to 11 show the CPA pure compound parameters dependence with the alkyl chain length of the substituent group in the methylimidazolium ring.

It can be seen that for non-association, the a_0 parameter can be considered constant, approximately 25 Pa m^6 mol^{-2}. For scheme 2B the a_0 parameter is not constant and for scheme 4C it is observed a slight decrease with the increase of the alkyl chain length. Considering scheme 1A, a linear behaviour can be observed.

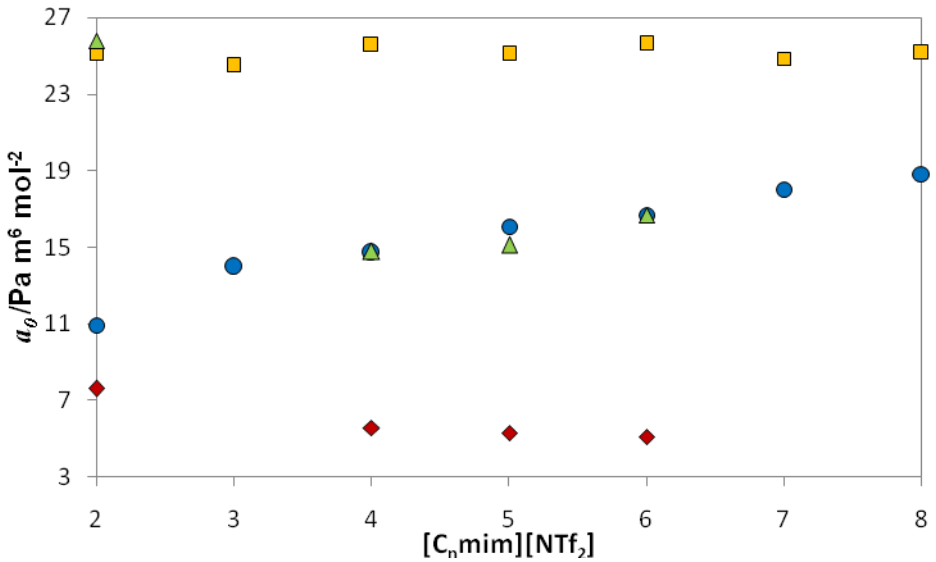

Figure 7 a_0 parameter values dependence with alkyl chain length (n), for non-association (■), 1A (●), 2B (▲) and 4C (◆) schemes association.

Comparing c_1 estimated values, it can be observed that does not exist a specific particular behaviour, for the different schemes considered, with the alkyl chain length (Figure 8).

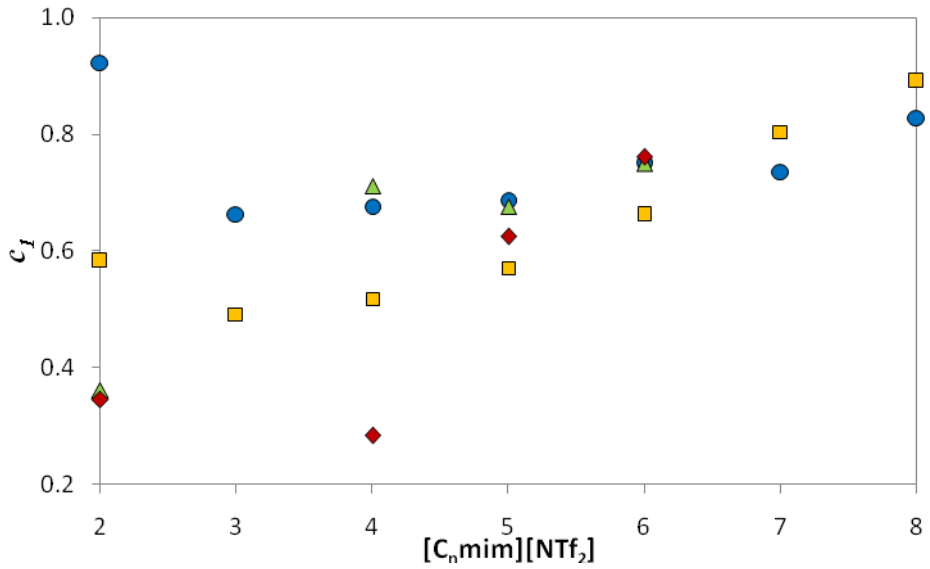

Figure 8 c_1 parameter values dependence with alkyl chain length (n), for non-association (■), 1A (●), 2B (▲) and 4C (◆) schemes association.

b estimated values, for the diverse studied association and non-association schemes, present a linear dependence with the alkyl chain length (Figure 9), except for [C_2mim][NTf_2] presenting higher values which might be explained due to the vapour pressure parameters which also do not present the same linear behaviour for n=2 as for the other ionic liquids (n=4, 6 and 8). This linear dependence is also seen for other compounds such as alkanes [57].

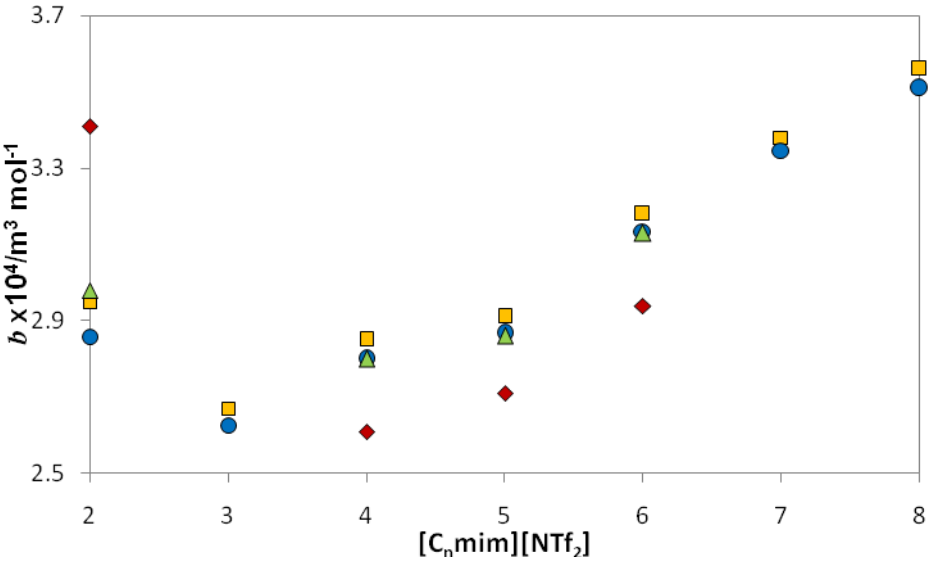

Figure 9 b parameter values dependence with alkyl chain length (n), for non-association (■), 1A (●), 2B (▲) and 4C (◆) schemes association.

The parameters of associating term are represented in Figure 10 and 11. For schemes 1A and 4C, the parameters values can be considered constant and alkyl chain length independent. The same is not observed for the 2B scheme, where the alkyl chain length is more influent.

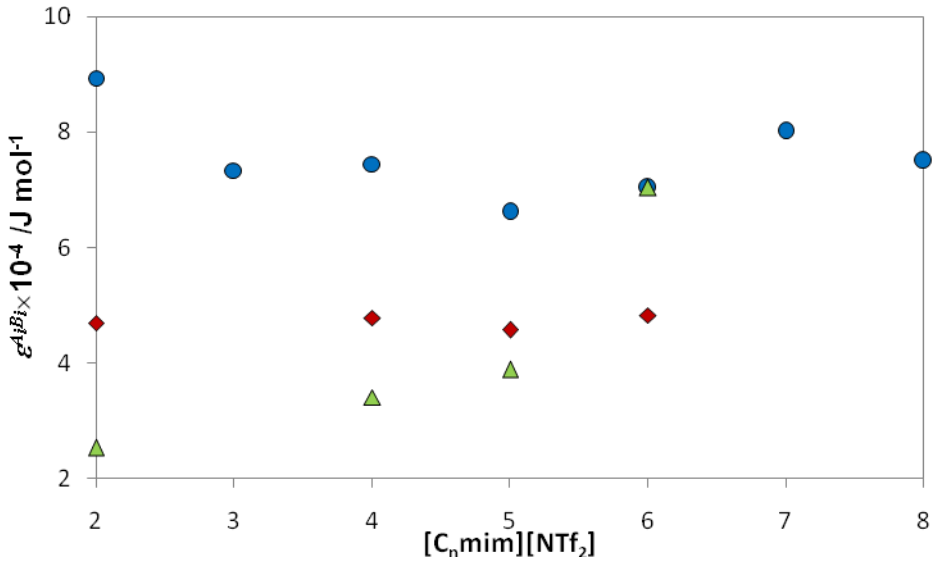

Figure 10 $\varepsilon^{A_iB_i}$ parameter values dependence with alkyl chain length (n), for 1A (●), 2B (▲) and 4C (◆) schemes association.

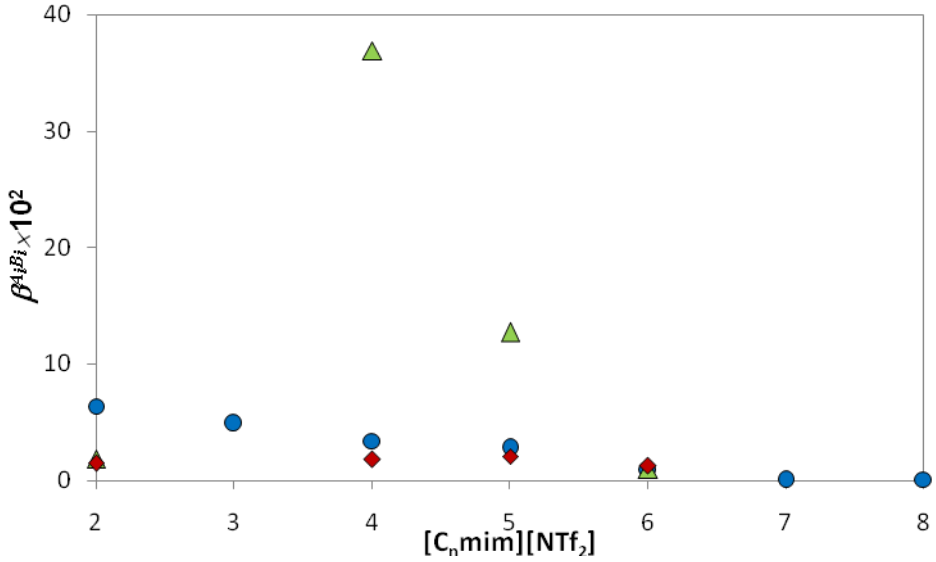

Figure 11 $\beta^{A_iB_i}$ parameter values dependence with alkyl chain length (n), for 1A (●), 2B (▲) and 4C (◆) schemes association.

A brief comparison between the alkyl chain length dependence (LD) and values (V) of the five pure compound parameters estimated for the $[C_n mim][NTf_2]$ family with the parameters obtained for other compounds is presented in Table 10.

Table 10 Comparison between CPA pure compounds parameters of $[C_n mim][NTf_2]$ and other compounds depending on the association scheme considered.

Association scheme	ILs compared with:	a_0		c_1		b		$\varepsilon^{A_i B_i}$		$\beta^{A_i B_i}$	
		LD	V	LD	V	LD	V	LD	V	LD	V
1A	Acids [49]	≈	>>	≈	≈	≈	≈	≈	>>	≠	≈
2B	Alcohol [43]	≠	>>>	≈	<	≠	≈	≠	>	≠	>
4C	Glycol [43]	≠	>	≠	≈	≠	≈	≈	>	>	≈
Non association	Alkanes [57]	≠	>>>	≈	≈	≈	≈	—	—	—	—

Symbols: ≠ different; ≈ similar; < smaller; > higher.

2.2.3 Correlation of the vapour–liquid equilibrium (VLE)

The description of the vapour-liquid phase equilibrium was performed for $[C_2mim][NTf_2]+CO_2$ and $[C_4mim][NTf_2]+CO_2$ systems by modelling the experimental data using the CPA EoS and the pure compounds parameters estimated in the previous section, where one binary interaction parameter, k_{ij}, was adjusted.

The experimental vapour-liquid equilibrium data of $[C_2mim][NTf_2]+CO_2$ system were obtained from the literature [7] and for $[C_4mim][NTf_2]+CO_2$ system were previously measured by Pedro Carvalho from this research group (PATh) and still remain unpublished.

The global average deviation (%AAD) for vapour-liquid equilibrium is calculated by:

$$\%AAD = \frac{1}{NP}\sum_{i=1}^{NP} ABS\left[\frac{x_{\exp,i} - x_{calc,i}}{x_{\exp,i}}\right] \times 100, \quad (23)$$

where x is the mole fraction.

An interaction parameter is needed to obtain a better vapour-liquid description as can be seen in Figure 12, where the %AAD is slightly higher when $k_{ij} = 0$ (Table 11), being this more significant for higher temperatures. The study of k_{ij} influence was made only for some temperatures for the [C_2mim][NTf_2]+CO_2 system, considering ionic liquids as non-associating compounds.

Table 11 CPA VLE results for [C_2mim][NTf_2]+CO_2 systems considering non-association for $k_{ij} = 0$ and $k_{ij} \neq 0$.

Temperature/K	%AAD	
	$k_{ij} = 0$	$k_{ij} \neq 0$ (Table 12)
293.04	22.94	16.56
323.16	18.70	15.84
353.11	23.00	9.56

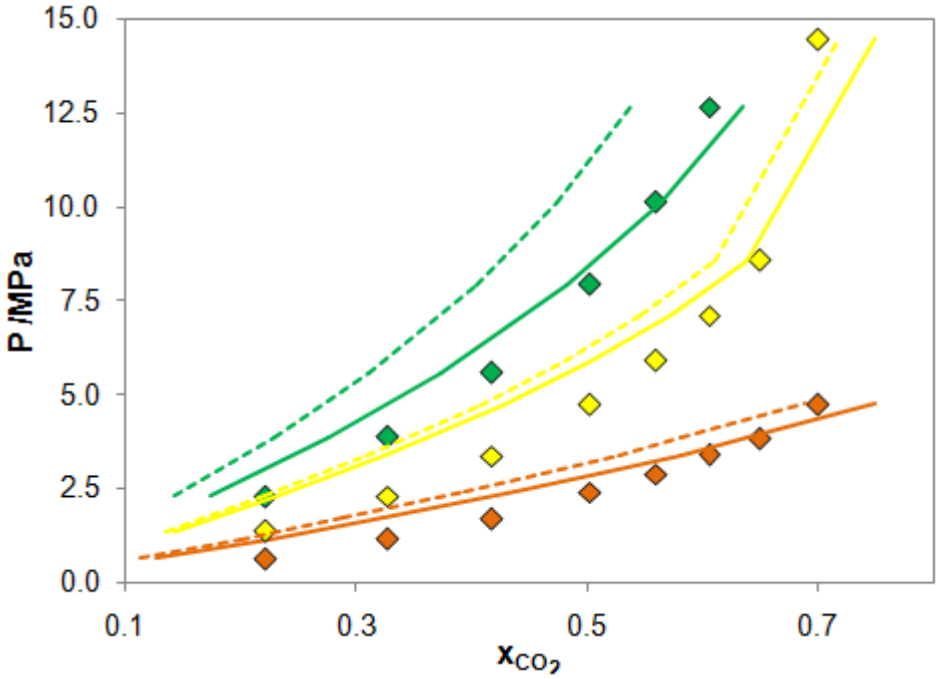

Figure 12 VLE Experimental data of [C_2mim][NTf_2]+CO_2 and CPA predictions for non-association for T=293.04K(◆), T=323.16(◆) and T=353.11(◆) with *kij*=0 (---) and *kij*=-0.016, -0.009 and -0.037, respectively (—).

Table 12 and Table 13 summarize the interaction parameters and the global average deviations between the CPA modelling results and the VLE experimental data of $[C_2mim][NTf_2]+CO_2$ system at temperatures between 293.04-353.11K, and $[C_4mim][NTf_2]+CO_2$ system at temperatures between 293.25-353.15K.

Global average deviations for both approaches are around or inferior to 20%, which for %AAD in composition are acceptable. Thus the results show that the CPA EoS has a good performance for describing CO_2+ionic liquids mixtures.

Table 12 CPA VLE results for $[C_2mim][NTf_2]+CO_2$ systems and binary interaction parameters considering non association and scheme 2B.

Temperature/K	k_{ij}		%AAD	
	Non-association	2B	Non-association	2B
293.04	-0.016	-0.022	16.56	16.08
298.26	-0.014	-0.019	16.32	15.55
303.36	-0.011	-0.015	16.57	16.28
313.31	-0.007	-0.012	16.96	16.36
323.16	-0.009	-0.013	15.84	15.18
333.11	-0.024	-0.029	11.61	15.89
343.20	-0.026	-0.031	11.08	10.69
353.11	-0.037	-0.042	9.56	9.26
Global %AAD			14.31	13.83

Table 13 CPA VLE results for $[C_4mim][NTf_2]+CO_2$ systems and binary interaction parameters considering non association and scheme 2B.

Temperature/K	k_{ij}		%AAD	
	Non-association	2B	Non-association	2B
293.25	-0.035	-0.028	22.17	22.74
303.18	-0.033	-0.021	20.95	21.68
313.19	-0.031	-0.015	21.23	22.08
323.19	-0.034	-0.016	19.81	20.61
333.18	-0.038	-0.018	18.71	19.43
343.10	-0.068	-0.052	11.34	11.72
353.15	-0.072	-0.055	10.83	11.25
Global %AAD			17.86	18.50

In Figure 13 and Figure 14, experimental data and CPA EoS correlation for vapour-liquid equilibrium is shown for non-association and association scheme 2B, for $[C_2mim][NTf_2]+CO_2$ and $[C_4mim][NTf_2]+CO_2$ systems, respectively. It was found a good agreement between the experimental data and the model, being a better description achieved for intermediate compositions. These figures also show that the improvement considering non-association or association scheme 2B is almost insignificant.

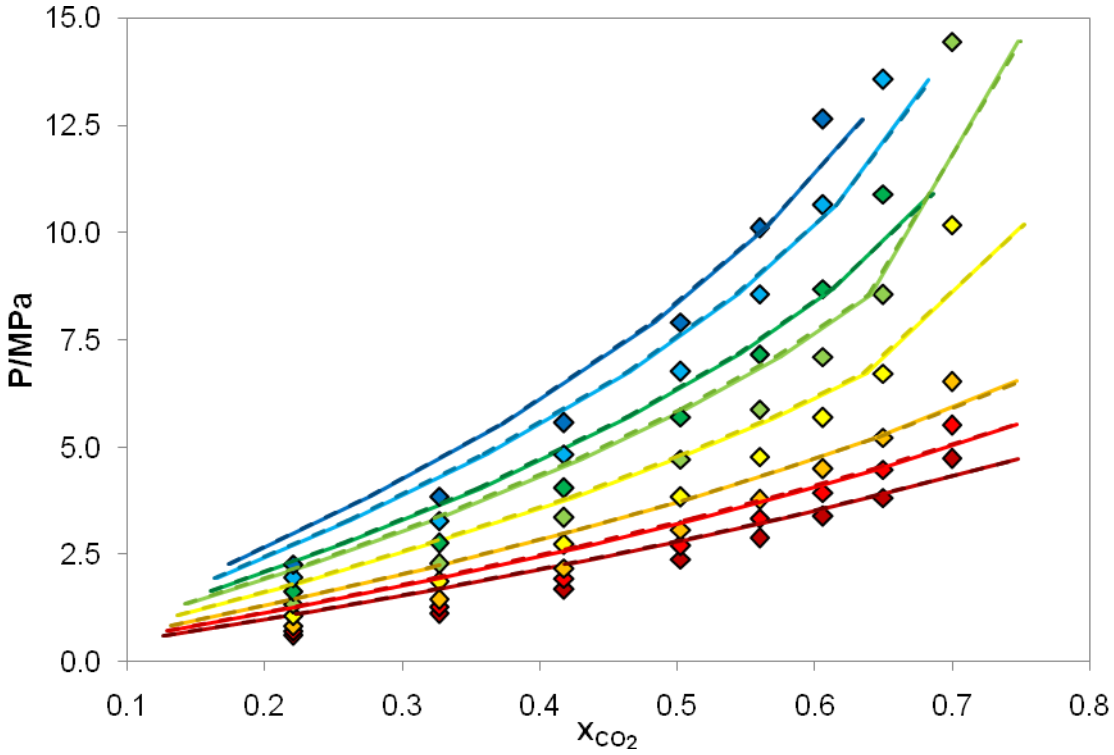

Figure 13 VLE Experimental data of $[C_2mim][NTf_2]+CO_2$ and CPA predictions for scheme 2B (—) and non-association (---), for T=293.04 K (◆), T=298.26 K (◆), T=303.36 K (◆), T=313.31 K (◆), T=323.16 K (◆), T=333.11 K (◆), T=343.20 K (◆) and T=353.11 K (◆).

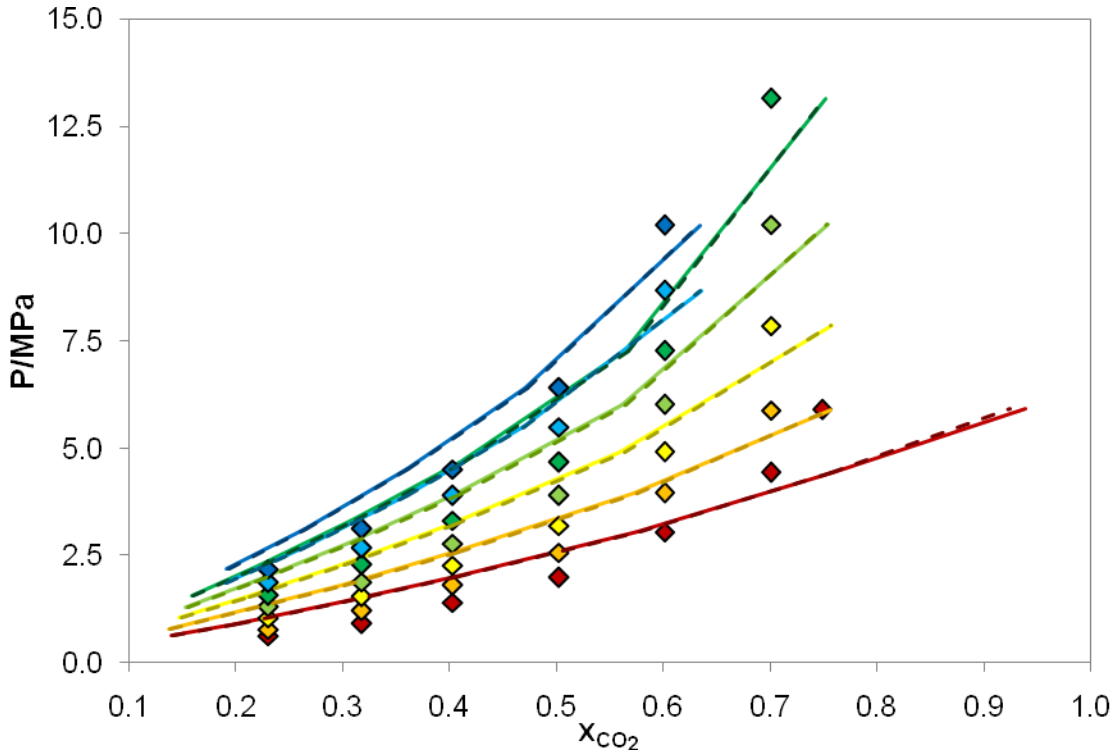

Figure 14 VLE Experimental data of $[C_4mim][NTf_2]+CO_2$ and CPA predictions for scheme 2B (—) and non-association (---), for T=293.25 K (◆), T=303.18 K (◆), T=313.18 K (◆), T=323.19 K (◆), T=333.18 K (◆), T=343.20 K (◆) and T=353.15 K (◆).

The k_{ij} parameters are temperature dependent, presenting an analogous behaviour for non-association and scheme 2B and for both systems studied. The difference between the schemes is similar in the range of temperature studied for $[C_2mim][NTf_2]+CO_2$ system, being a little higher for $[C_4mim][NTf_2]+CO_2$ (see Figure 15 and Figure 16). The lower absolute values are observed for lower temperatures, and when non-association is considered for $[C_2mim][NTf_2]+CO_2$ systems, and scheme 2B for $[C_4mim][NTf_2]+CO_2$ systems.

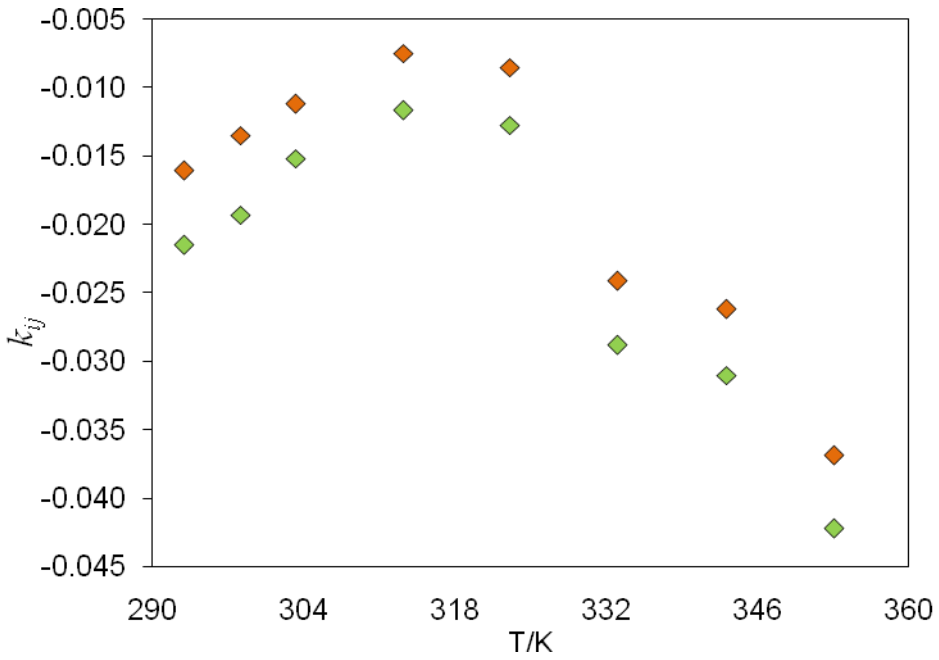

Figure 15 Interaction parameters dependence with temperature, with non-association (◆) and for scheme 2B (◆), for $[C_2mim][NTf_2]+CO_2$ systems.

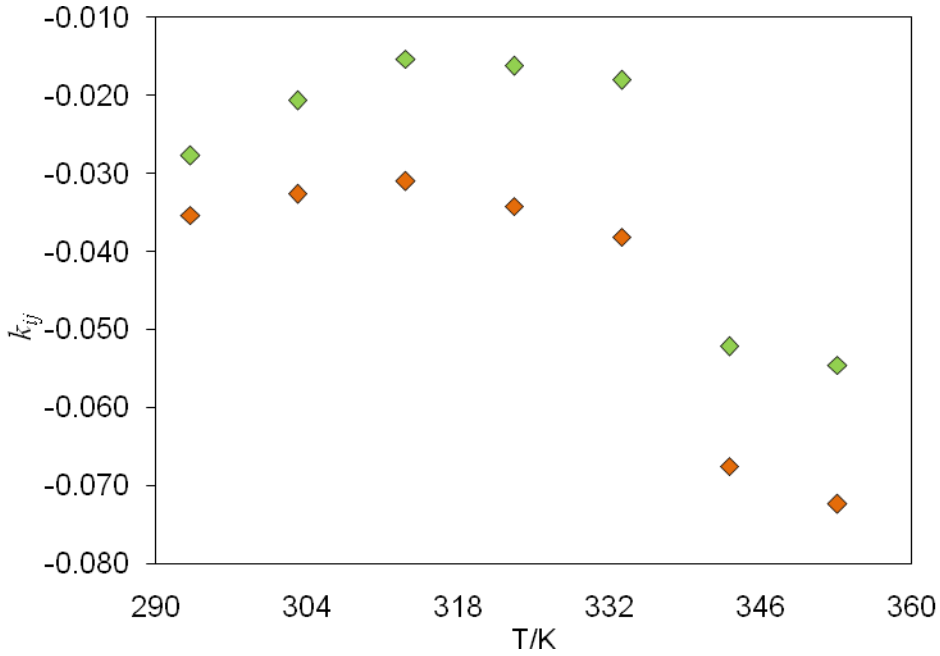

Figure 16 Interaction parameters dependence with temperature, with non-association (◆) and for scheme 2B (◆), for $[C_4mim][NTf_2]+CO_2$ systems.

It can be seen that the scheme with lower k_{ij} absolute values, is the scheme that better describes the VLE experimental data, despite the very small difference between %AAD obtained for each scheme.

Another approach was to use a single binary interaction parameter for modelling these VLE experimental data, for all temperatures. The results show that, for the 2B association scheme, only one k_{ij} parameter is needed to obtain a good description of the model, due to the lower Global %AAD difference observed, which can be seen, by comparison, in Tables 12, 13 and 14. Therefore these results can suggest that the CPA EoS can be used as a predictive tool, with a small and temperature independent binary interaction parameter.

Table 14 CPA VLE results for $[C_2mim][NTf_2]+CO_2$ and $[C_4mim][NTf_2]+CO_2$ systems and binary interaction parameters.

System	Global k_{ij}		Global %AAD	
	Non-association	2B	Non-association	2B
$[C_2mim][NTf_2]+CO_2$	-0.013	-0.017	16.34	14.54
$[C_4mim][NTf_2]+CO_2$	-0.036	-0.021	20.88	23.33

For the 1A and 4C schemes it was not achieved any acceptable results due to the non convergence of the phase equilibrium calculations routine which leads to the assumption that these schemes cannot describe this equilibrium.

3. EXPERIMENTAL MEASUREMENTS AND CPA MODELLING

With the aim of further understanding the interactions between CO_2 and solvents, carbon dioxide solubility in carbon disulphide and carbon tetrachloride were also studied.

Carbon disulphide and carbon tetrachloride were chosen duo the similar geometric structure to carbon dioxide and methane, respectively, and the influence that the change of some atoms in the solvent molecule can have in the solubility.

Due to the lack of experimental data for these systems, carbon dioxide solubility measurements were performed in a high pressure cell.

3.1 Materials

The chemicals used for the measurements were carbon disulphide, carbon tetrachloride and carbon dioxide. Carbon disulphide was acquired from Panreac with mass fraction purities 99.9 % and Carbon tetrachloride was acquired from SDS with mass fraction purities 99.9 %.

The carbon dioxide used was from Air Liquide with a purity of ≥ 99.998 % and H_2O, O_2, C_nH_m, N_2 and H_2 impurities volume fractions lower than (3, 2, 2, 8 and 0.5)$\times 10^{-6}$, respectively.

3.2 Experimental Apparatus and Procedure

Solubility measurements were carried out in a high pressure equilibrium cell (Figure 17) using a visual synthetic method, sketched in Figure 18.

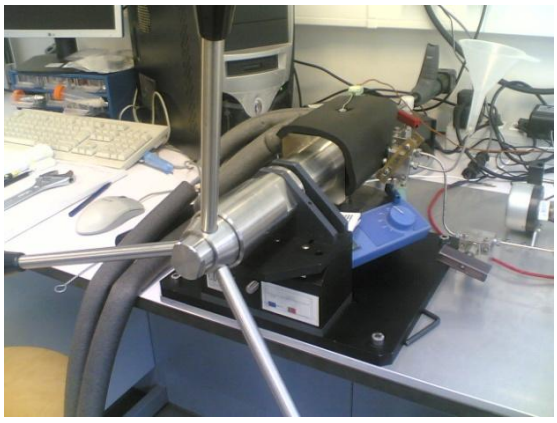

Figure 17 High pressure cell.

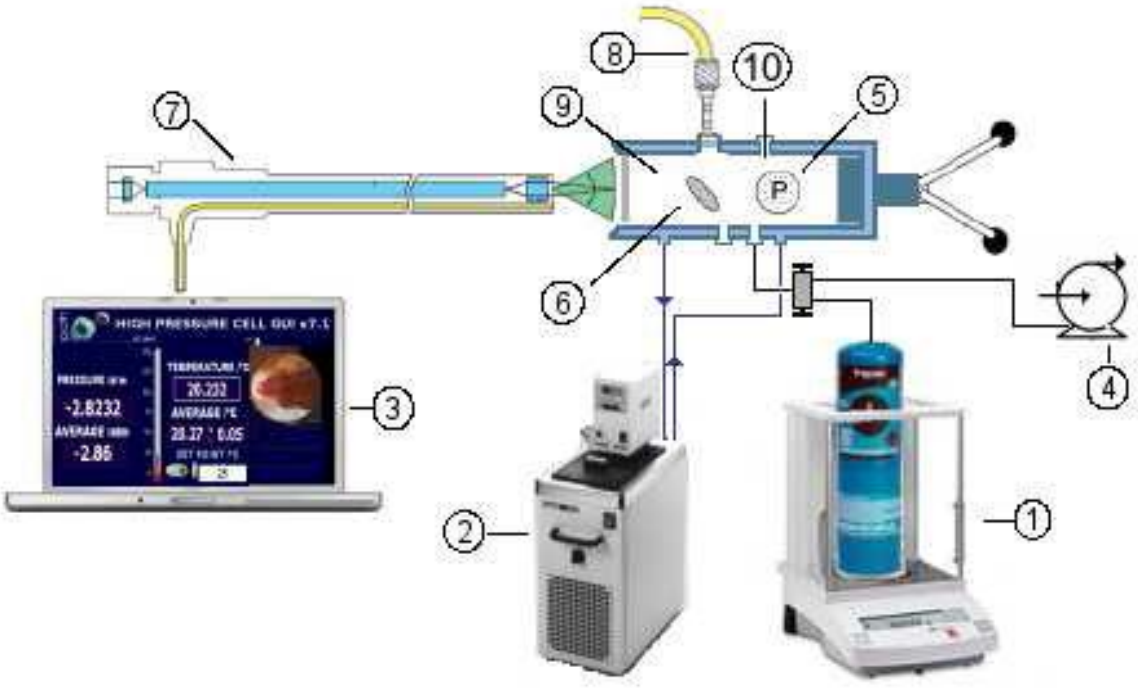

Figure 18 Schematic apparatus: 1 – analytical balance; 2 – thermostat bath circulator; 3 – computer for data and video acquisition; 4 – vacuum pump; 5 – piezoresistive silicon pressure transducer; 6 – magnetic bar; 7 – endoscope plus a video camera; 8 – light source with optical fiber cable; 9 – high pressure variable-volume cell; 10 – temperature probe.

The cell, based on the design of Daridon et al. [7], consists of a horizontal hollow stainless-steel cylinder, closed in the extremes by a movable piston and a sapphire window, there is another sapphire window in the cell wall. These windows allow an optical fiber to illuminate the cell chamber and the visual observation of what happens inside the measuring cell, which is achieved by a video acquisition system made up of an endoscope plus a video camera placed behind one of the sapphire windows in order to display on the screen of a computer. The orthogonal positioning of both sapphire windows minimizes the parasitic reflections and improves the observation in comparison to axial lighting.

The mixture homogenization is ensured by a small magnetic bar placed inside the cell by means of an external magnetic stirrer.

The sapphire windows on the cell wall and the magnetic bar limit the minimum internal volume of the cell to 8 cm^3, while the maximum value is fixed to 30 cm^3. The presence of the magnetic stirrer, as well as the cell reduced volume, help to minimize the inertia and temperature gradients within the sample.

The cell is thermostatized by circulating a heat-carrier fluid, thermo-regulated with a temperature stability of ±0.01 K by means of a thermostat bath circulator (Julabo MC), through three flow lines directly managed into the cell. The temperature is measured with a high precision thermometer, Model PN 5207 with an accuracy of 0.01 K, connected to a calibrated platinum resistance inserted inside the cell close to the sample.

The pressure is measured by a piezoresistive silicon pressure transducer (Kulite) fixed directly inside the cell to reduce dead volumes, that was previously calibrated and certified by an independent laboratory with IPAC accreditation, following the EN 837-1 standard and with accuracy better than 0.2 %.

A fixed amount of liquid was introduced inside the cell and the exact mass introduced is determined by weighting the liquid holder during its introduction with a precision balance (Sartorius) with an accuracy of 1 mg.

The CO_2 was introduced under pressure from an aluminum reservoir tank. Its mass was measured with the precision balance by weighing the reservoir tank while filling and introduced into the measuring cell by means of a flexible high pressure capillary.

After preparation of a mixture of known composition at the desired temperature at low pressure was reached, the pressure was then slowly increased at constant temperature until the system becomes monophasic. The pressure at which the last bubble disappears represents the equilibrium pressure (bubble pressure) for the fixed temperature.

3.3 Experimental Data

The solubility of carbon dioxide in carbon tetrachloride was measured for mole fraction from 0.16 to 0.70, for 293.22, 313.26 and 333.22 K, and pressures from 1.09 to 7.85 MPa, and is reported in Table 15.

Table 15 Experimental solubility data of carbon dioxide in carbon tetrachloride (CCl_4) for different CO_2 mole fractions and for 293.22, 313.26 and 333.22 K.

Temperature/K					
293.22		313.26		333.22	
x_{CO_2}	P/MPa	x_{CO_2}	P/MPa	x_{CO_2}	P/MPa
0.16	1.09	0.16	1.57	0.16	2.10
0.20	1.38	0.20	2.00	0.20	2.67
0.30	2.04	0.30	2.93	0.30	3.87
0.40	2.61	0.40	3.79	0.40	5.02
0.50	3.07	0.50	4.49	0.50	6.04
0.60	3.51	0.60	5.15	0.60	7.02
0.70	3.84	0.70	5.73	0.70	7.85

The solubility of carbon dioxide in carbon disulphide was measured for mole fraction from 0.05 to 0.60, for 293.27, 313.26 and 333.13 K, and pressures from 0.97 to 8.52 MPa, and is reported in Table 16.

Table 16 Experimental solubility data of carbon dioxide in carbon disulphide (CS_2) for different CO_2 mole fractions and for 293.27, 313.26 and 333.13 K.

Temperature/K					
293.27		313.26		333.13	
x_{CO_2}	P/MPa	x_{CO_2}	P/MPa	x_{CO_2}	P/MPa
0.05	0.97	0.05	1.36	0.05	1.75
0.10	1.93	0.10	2.55	0.10	3.18
0.20	3.22	0.20	4.34	0.20	5.44
0.30	3.87	0.30	5.37	0.30	6.92
0.40	4.09	0.40	5.90	0.40	7.81
0.50	4.13	0.50	6.11	0.50	8.30
0.60	4.07	0.60	6.12	0.60	8.52

In Figure 19 and Figure 20, carbon dioxide solubility behaviour in temperature and pressure is presented. As can be seen, solubility of carbon dioxide in this solvents increase with increasing pressure and decreases with increasing temperature. For the CCl_4+CO_2 system, an almost linear depence with the composition can be seen. For the

CS_2+CO_2 system a linear dependence only can be seen for the lowest concentrations of carbon dioxide.

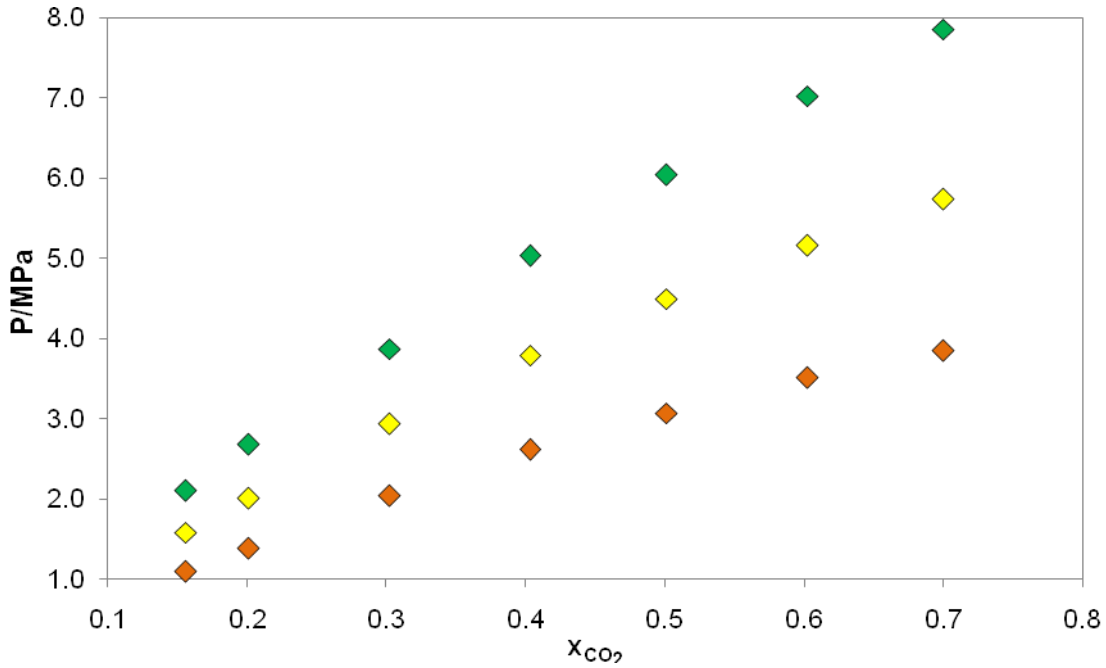

Figure 19 Experimental solubility data for CO_2 in CCl_4 for T=293.22 K (◆), T=313.26 K (◆) and T=333.22 K (◆).

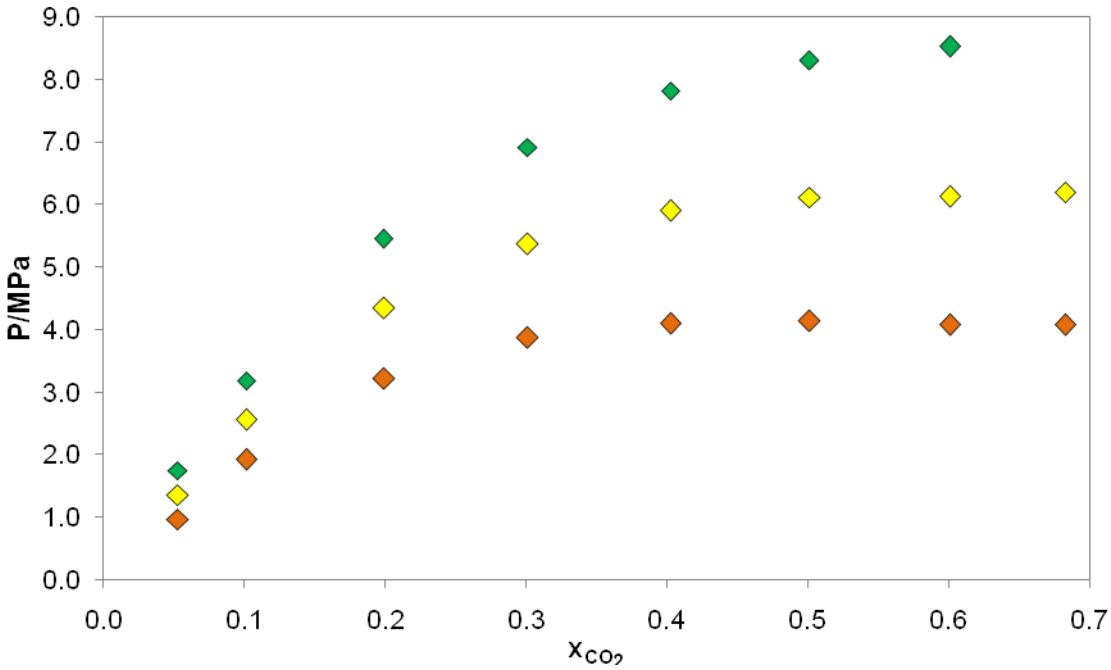

Figure 20 Experimental solubility data for CO_2 in CS_2 for T=293.27 K (◆), T=313.26 K (◆) and T=333.13 K (◆).

3.4 Experimental data modelling with CPA

The experimental carbon dioxide solubility data in carbon tetrachloride and carbon disulphide were also modelled with the CPA EoS.

3.4.1 Compilation and selection of available data

Vapour pressure, liquid density, and critical properties were also required and obtained from the DIPPR database [51] (Equation 19, Equation 20, Table A1, Table B 1 and Table B 2).

The reduced temperature range covered for carbon tetrachloride and carbon disulphide was from 0.45 to 0.85.

3.4.2 Correlation of the CPA pure compound parameters

Carbon disulphide (as carbon dioxide in this work) and carbon tetrachloride (as methane [44], which as similar structure having different volume and electronegative due to hydrogen atoms substitution by chlorine atoms) were considered non self-associating compounds, thus only three CPA parameters were required (Table 17). It was achieved a very good description of vapour pressure and liquid density with very low values obtained for %AAD.

Table 17 CPA pure compound parameters and modelling results for CO_2, CS_2, CCl4 and CH_4.

Compound	a_0 (Pa m^6 mol^{-2})	c_1	$b\times10^5$ (m^3 mol^{-1})	%AAD P^σ	%AAD $\rho^{liq.}$
CO_2	0.35	0.76	2.72	0.22	0.83
CS_2	1.14	0.60	4.95	0.76	0.74
CCl_4	1.90	0.74	8.10	1.01	0.63

Comparing the parameters of carbon dioxide, carbon disulphide and carbon tetrachloride, it can be seen that the parameters a_0 and b are higher for CS_2 and for CCl_4 than for CO_2 and the c_1 parameter variation is very small. Thus the parameters a_0 and b vary more than the parameter c_1 for the different compounds.

The results obtained for these molecules can be due to the increase of the molecule size and weight mass and influenced by the critical temperature.

3.4.3 Correlation of the vapour–liquid equilibrium (VLE)

VLE modelling results for CCl_4+CO_2 and CS_2+CO_2 are presented below.

► *CCl_4+CO_2 system*

In Figure 21, experimental data and CPA EoS correlation of vapour-liquid equilibrium (solubility) is shown. It can be seen that a great agreement was achieved with global average deviation of 3.94% in composition, with small and positive binary interaction parameters (Table 18). An improved description is achieved for lower CO_2 mole fraction.

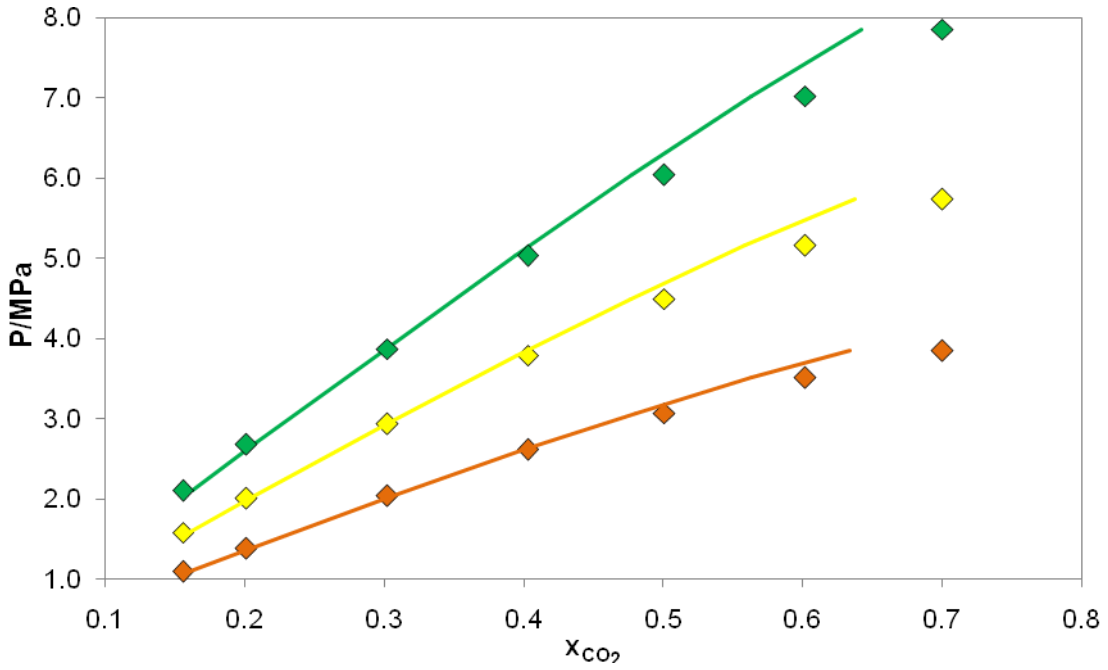

Figure 21 Experimental solubility data for CO_2 in CCl_4 for T=293.22 K (◆), T=313.26 K (◆) and T=333.22 K (◆) and CPA predictions (—) with non-association.

Table 18 CPA VLE results for CCl_4+CO_2 system and binary interaction parameters with non-association.

Temperature/K	k_{ij}	%AAD
293.22	0.075	3.81
313.26	0.087	3.89
333.22	0.093	4.13
Global %AAD		3.94

k_{ij} values versus temperature are represented in Figure 22, where a linear dependence with temperature can be seen.

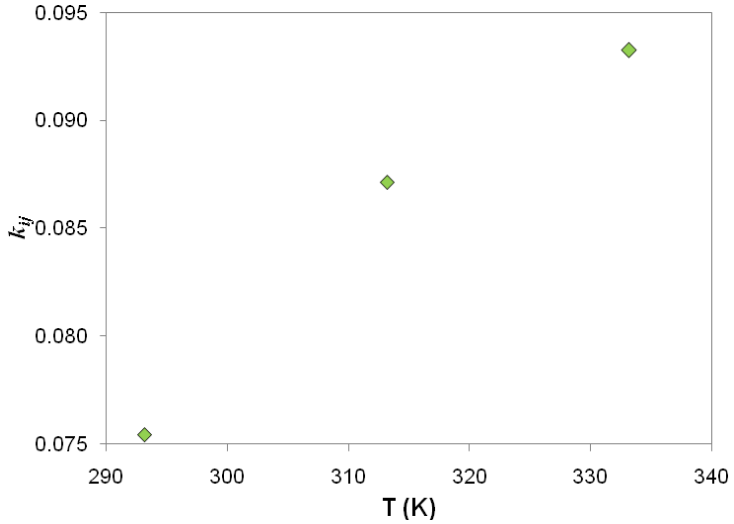

Figure 22 Binary interaction parameters dependence with temperature, with non-association for CCl_4+CO_2 system.

► *CS_2+CO_2 system*

The modelling results obtained for this system, using the CPA parameters estimated by vapour pressure and liquid density experimental data, for 293.27 K and for 333.13 K were not very good. So, in order to get better results, CPA modelling was done using the compound critical properties for 313.26 K and 333.13 K. Comparing the model description for 333.13 K, a better result is obtained when the critical properties are used. These observations can be seen in Figure 23, being supported by the %AAD and k_{ij} values, shown in Table 19, which are higher than the obtained for CO_2+CCl_4 systems.

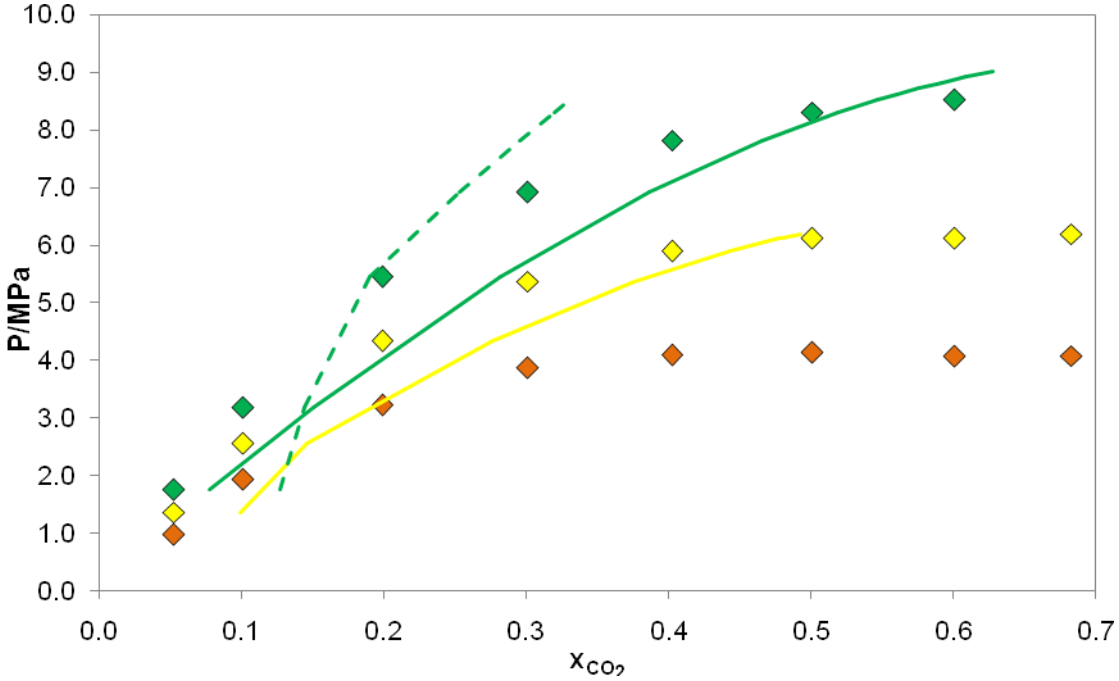

Figure 23 Experimental solubility data for CO_2 in CS_2 for T=293.27K (◆), T=313.26K (◆) and T=333.13K (◆) and CPA predictions with non-association for vapour pressure and liquid density experimental data fitting (---) and using critical properties (—).

Table 19 CPA VLE results for CS_2+CO_2 system and binary interaction parameters with non-association.

Approach	Temperature/K	k_{ij}	%AAD
Using Critical Properties	313.26	0.11	32.37
	333.13	0.10	27.89
Using fitted parameters	333.13	0.18	44.58

These bad results might be associated to deficient experimental data; therefore CS_2+CO_2 vapour-liquid equilibrium must be measured once again.

4. CONCLUSIONS

Due to environmental issues originated by carbon dioxide emissions, its capture has become critical and the processes employed are being improved and new processes developed.

Ionic liquids are one of the new sorbents investigated for carbon dioxide capture, being the solubility of carbon dioxide in some of these fluids higher than in conventional solvents. Another important improvement obtained by using these solvents, due to their negligible vapour pressure, is the possible replacement of volatile organic compounds (VOCs) which are prejudicial to Man and the environment.

Due to the increasing utilization of ionic liquids in chemical and industrial processes, it is necessary to develop correlations and predictive models able to describe behaviours and properties.

Several models have already been applied to describe vapour-liquid equilibrium data of carbon dioxide and ionic liquids systems, being for the first time, in this work, the Cubic Plus Association equation of state applied (CPA EoS), where 1A, 2B and 4C association schemes and non-association were studied.

CPA parameters were estimated by fitting vapour pressure and liquid density experimental data for the $[C_n mim][NTf_2]$ ionic liquids selected and carbon dioxide and good results were achieved with global deviation in vapour pressure and liquid density inferior to 1% when association is considered for ionic liquids.

$[C_2 mim][NTf_2]+CO_2$ and $[C_4 mim][NTf_2] +CO_2$ vapour-liquid experimental data were modelled and successful results were achieved, considering carbon dioxide a non-associating compound and the ionic liquids as non associating and auto associating compounds (scheme 2B), with global deviations in composition inferior to 20%. The global deviation difference obtained for both cases is very low thus the use of the association does not improve the performance of the CPA EoS. A good description of vapour-liquid equilibrium data of the systems studied was also possible with a single temperature independent binary interaction parameter.

In addition, carbon dioxide solubility in carbon disulphide and in carbon tetrachloride were measured in a high pressure cell and also modelled with the CPA EoS. Carbon dioxide solubility increase with increasing pressure and decreases with increasing temperature, and was found to be higher in carbon tetrachloride than in carbon disulphide. The CPA modelling results of the CO_2+CCl_4 system achieved had a very good agreement with the experimental data, with global deviations in carbon dioxide composition equal to 3.94%, but for the CO_2+CS_2 system results were not that good, being necessary another approach, with better results, that is the modelling using the critical properties.

Due to the very satisfactory results obtained, the CPA EoS is a useful and satisfactory model to accurately describe the vapour-liquid equilibrium of CO_2 systems.

Future work:

- CPA pure compound parameters optimization (try to reduce its values) and use constant values for them for all the ionic liquids, to obtain improved modelling results with CPA.
- Vapour-liquid equilibrium experimental data modelling with constant CPA pure compound parameters and temperature independent binary interaction parameters for the $[C_n mim][NTf_2]$ ionic liquid family.
- SRK EoS (reduced CPA EoS, using the critical properties) modelling with the aim to compare the results obtained by vapour pressure and liquid density experimental data fitting and the ones by the use of the critical properties.
- Phase equilibrium measurements and CPA modelling for other carbon dioxide + ionic liquids systems in order to find selective ionic liquids, or ionic liquids mixtures, that improve carbon dioxide solubility.
- Additional solubility measurements of carbon dioxide and carbon disulphide to confirm the experimental data presented in this work, and its modelling.
- Solubility measurements of other compounds usually associated to gas mixtures in ionic liquids and carbon dioxide, to obtain more useful data for chemical and industrial processes.

5. BIBLIOGRAPHIC REFERENCES

1. Hardy, J.T., *Climate Change: Causes, Effects and Solutions*. 2003, Chichester: Wiley

2. Abu-Khader, M.M., *Recent progress in CO2 capture/sequestration: A review. Energy Sources Part a-Recovery Utilization and Environmental Effects*, 2006. **28**(14): p. 1261-1279.

3. Figueroa, J.D., Fout, T., Plasynski, S., McIlvried, H., and Srivastava, R.D., *Advances in CO2 capture technology - The US Department of Energy's Carbon Sequestration Program*. International Journal of Greenhouse Gas Control, 2008. **2**(1): p. 9-20.

4. Plasynski, S.I., Litynski, J.T., McIlvried, H.G., and Srivastava, R.D., *Progress and New Developments in Carbon Capture and Storage.* Critical Reviews in Plant Sciences, 2009. **28**(3): p. 123-138.

5. Perinline, H.W., Luebke, D.R., Jones, K.L., Myers, C.R., Morsi, B.I., Heintz, Y.J., and Ilconich, J.B., *Progress in carbon dioxide capture and separation research for gasification-based power generation point sources.* Fuel Processing Technology, 2008. **89**(9): p. 897-907.

6. El Seoud, O.A., Koschella, A., Fidale, L.C., Dorn, S., and Heinze, T., *Applications of ionic liquids in carbohydrate chemistry: A window of opportunities.* Biomacromolecules, 2007. **8**(9): p. 2629-2647.

7. Carvalho, P.J., Alvarez, V.H., Machado, J.J.B., Pauly, J., Daridon, J.L., Marrucho, I.M., Aznar, M., and Coutinho, J.A.P., *High pressure phase behavior of carbon dioxide in 1-alkyl-3-methylimidazolium bis(trifluoromethylsulfonyl)imide ionic liquids.* Journal of Supercritical Fluids, 2009. **48**(2): p. 99-107.

8. Stracke, M.P., Migliorini, M.V., Lissner, E., Schrekker, H.S., Dupont, J., and Goncalves, R.S., *Imidazolium ionic liquids as electrolytes for manganese dioxide free Leclanche batteries.* Applied Energy, 2009. **86**(9): p. 1512-1516.

9. Lu, J.M., Yan, F., and Texter, J., *Advanced applications of ionic liquids in polymer science.* Progress in Polymer Science, 2009. **34**(5): p. 431-448.

10. Wuebbles, D.J.E., J., *Primer on Green Gases.* 1991, Michigan: Lewis Publishers,Inc.

11. Watts, R.G., ed. *Engineering Response to Global Climate Change: Planning a Research and Development Agenda.* 2000, CRC Press LLC: United States of America.

12. Kondratyev, K.Y.C., A. P., *Observing Global Climate Change*. 1998, St. Petersburg: Taylor & Francis Ltd.

13. Burroughs, W.J., *Climate Change: A multidisciplinary Approach.* 2007, Cambridge: University Press.

14. I.P.o.C.C., http://www.ipcc.ch/graphics/index.htm.(14-05-09)

15. EIA, 2006, http://www.eia.doe.gov/oiaf/1605/ggrpt/carbon.html#total. (13-05-09)

16. http://www.epa.gov/climatechange/emissions/co2_human.html. (13-05-09)

17. Yang, H.Q., Xu, Z.H., Fan, M.H., Gupta, R., Slimane, R.B., Bland, A.E., and Wright, I., *Progress in carbon dioxide separation and capture: A review*. Journal of Environmental Sciences-China, 2008. **20**(1): p. 14-27.

18. *New CO2 capture technology advances*. Chemical & Engineering News, 2008. **86**(37): p. 30-30.

19. Gibbins, J. and Chalmers, H., *Carbon capture and storage*. Energy Policy, 2008. **36**(12): p. 4317-4322.

20. Lackner, K.S., *A guide to CO2 sequestration. Science*, 2003. **300**(5626): p. 1677-1678.

21. CCP, 2008, http://www.co2captureproject.org/about_capture.html. (23-05-09)

22. Desideri, U., Arcioni, L., and Tozzi, M., *Feasibility study for a carbon capture and storage project in northern Italy*. International Journal of Energy Research, 2008. **32**(12): p. 1175-1183.

23. Paul, J.P., C., ed. Carbon Dioxide Chemistry: Environmental Issues. 1994, The Royal Society of Chemistry: Cambridge.

24. Karakatsani, E.K., Economou, L.G., Kroon, M.C., Peters, C.J., and Witkamp, G.J., T*PC-PSAFT modeling of gas solubility in imidazolium-based ionic liquids*. Journal of Physical Chemistry C, 2007. **111**: p. 15487-15492.

25. Pratas, M.J., *Medição da solubilidade de gases em líquidos iónicos com microbalança de cristais de quartzo*, in Departamento de Química., MSc Thesis, 2007, Universidade de Aveiro: Aveiro.

26. Anderson, J.L., Dixon, J.K., and Brennecke, J.F., *Solubility of CO2,CH4, C2H6, C2H4, O-2, and N-2 in 1-hexyl-3-methylpyridinium bis(trifluoromethylsulfonyl)imide: Comparison to other ionic liquids*. Accounts of Chemical Research, 2007. **40**: p. 1208-1216.

27. Krossing, I., Slattery, J.M., Daguenet, C., Dyson, P.J., Oleinikova, A., and Weingartner, H., *Why are ionic liquids liquid? A simple explanation based on lattice and solvation energies*. Journal of the American Chemical Society, 2006. **128**(41): p. 13427-13434.

28. Wang, T.F., Peng, C.J., Liu, H.L., and Hu, Y., *Description of the pVT behavior of ionic liquids and the solubility of gases in ionic liquids using an equation of state*. Fluid Phase Equilibria, 2006. **250**(1-2): p. 150-157.

29. Shiflett, M.B., Kasprzak, D.J., Junk, C.P., and Yokozeki, A., *Phase behavior of {carbon dioxide plus [bmim][Ac]} mixtures*. Journal of Chemical Thermodynamics, 2008. **40**(1): p. 25-31.

30. Dong, W.S., Lin, F.Q., Liu, C.L., and Li, M.Y., *Synthesis of ZrO2 nanowires by ionic-liquid route*. Journal of Colloid and Interface Science, 2009. **333**(2): p. 734-740.

31. Andreu, J.S. and Vega, L.F., *Capturing the solubility Behavior of CO2 in ionic liquids by a simple model*. Journal of Physical Chemistry C, 2007. **111**: p. 16028-16034.

32. Andreu, J.S. and Vega, L.F., *Modeling the Solubility Behavior of CO2, H-2, and Xe in [C-n-mim][Tf2N] Ionic Liquids*. Journal of Physical Chemistry B, 2008. **112**(48): p. 15398-15406.

33. Couling, D.J., Bernot, R.J., Docherty, K.M., Dixon, J.K., and Maginn, E.J., *Assessing the factors responsible for ionic liquid toxicity to aquatic organisms via quantitative structure-property relationship modeling*. Green Chemistry, 2006. **8**(1): p. 82-90.

34. Freire, M.G., Ventura, S.P.M., Santos, L., Marrucho, I.M., and Coutinho, J.A.P., *Evaluation of COSMO-RS for the prediction of LLE and VLE of water and ionic liquids binary systems*. Fluid Phase Equilibria, 2008. **268**(1-2): p. 74-84.

35. Raeissi, S. and Peters, C.J., *A potential ionic liquid for CO2-separating gas membranes: selection and gas solubility studies*. Green Chemistry, 2009. **11**(2): p. 185-192.

36. Muldoon, M.J., Aki, S., Anderson, J.L., Dixon, J.K., and Brennecke, J.F., *Improving carbon dioxide solubility in ionic liquids*. Journal of Physical Chemistry B, 2007. **111**(30): p. 9001-9009.

37. Kroon, M.C., Karakatsani, E.K., Economou, I.G., Witkamp, G.J., and Peters, C.J., *Modeling of the carbon dioxide solubility in imidazolium-based ionic liquids with the tPC-PSAFT equation of state*. Journal of Physical Chemistry B, 2006. **110**(18): p. 9262-9269.

38. Zhang, X.C., Liu, Z.P., and Wang, W.C., *Screening of ionic liquids to capture CO2 by COSMO-RS and experiments*. Aiche Journal, 2008. **54**(10): p. 2717-2728.

39. Wang, T.F., Peng, C.J., Liu, H.L., Hu, Y., and Jiang, J.W., *Equation of state for the vapor-liquid equilibria of binary systems containing imidazolium-based ionic liquids*. Industrial & Engineering Chemistry Research, 2007. **46**(12): p. 4323-4329.

40. Shiflett, M.B. and Yokozeki, A., *Solubility of CO2 in room temperature ionic liquid [hmim][Tf2N]*. Journal of Physical Chemistry B, 2007. **111**(8): p. 2070-2074.

41. Breure, B., Bottini, S.B., Witkamp, G.J., and Peters, C.J., *Thermodynamic modeling of the phase behavior of binary systems of ionic liquids and carbon dioxide with the group contribution equation of state*. Journal of Physical Chemistry B, 2007. **111**(51): p. 14265-14270.

42. Yuan, X.L., Zhang, S.J., Liu, J., and Lu, X.M., *Solubilities of CO2 in hydroxyl ammonium ionic liquids at elevated pressures*. Fluid Phase Equilibria, 2007. **257**(2): p. 195-200.

43. Kontogeorgis, G.M., Michelsen, M.L., Folas, G.K., Derawi, S., von Solms, N., and Stenby, E.H., *Ten years with the CPA (Cubic-Plus-Association) equation of state. Part 1. Pure compounds and self-associating systems*. Industrial & Engineering Chemistry Research, 2006. **45**(14): p. 4855-4868.

44. Oliveira, M.B., Coutinho, J.A.P., and Queimada, A.J., *Mutual solubilities of hydrocarbons and water with the CPA EoS*. Fluid Phase Equilibria, 2007. **258**(1): p. 58-66.

45. Oliveira, V.L.H., *Modelling the Aqueous Solubility of PAHs with CPA EoS*, in Departamento de Química., MSc Thesis, 2008, Universidade de Aveiro: Aveiro.

46. Fu, Y.H. and Sandler, S.I., A *simplified SAFTt equation of state for associating compounds and mixtures*. Industrial & Engineering Chemistry Research, 1995. **34**(5): p. 1897-1909.

47. Suresh, S.J. and Elliott, J.R., M*ultiphase equilibrium-analysis via a generalized equation of state for associating mixtures*. Industrial & Engineering Chemistry Research, 1992. **31**(12): p. 2783-2794.

48. Oliveira, M.B., Teles, A.R.R., Queimada, A.J., and Coutinho, J.A.P., *Phase equilibria of glycerol containing systems and their description with the Cubic-Plus-Association (CPA) Equation of State*. Fluid Phase Equilibria, 2009. **280** (1-2):p. 22-29.

49. Oliveira, M.B., Pratas, M.J., Marrucho, I.M., Queimada, A.J., and Coutinho, J.A.P., *Description of the Mutual Solubilities of Fatty Acids and Water With the CPA EoS*. Aiche Journal, 2009. **55**(6): p. 1604-1613.

50. Huang, S.H. and Radosz, M., *Equation of State for small, large, polydisperse and associating molecules*. 1990. **29**: p. 2284.

51. Design Institute for Physical Property Data, *DIPPR Database*. 1998, AIChE: New York.

52. Esperanca, J., Visak, Z.P., Plechkova, N.V., Seddon, K.R., Guedes, H.J.R., and Rebelo, L.P.N., *Density, speed of sound, and derived thermodynamic properties of ionic liquids over an extended pressure range. 4. [C(3)mim][NTf2] and [C(5)mim][NTf2]*. Journal of Chemical and Engineering Data, 2006. **51**(6): p. 2009-2015.

53. de Azevedo, R.G., Esperanca, J., Szydlowski, J., Visak, Z.P., Pires, P.F., Guedes, H.J.R., and Rebelo, L.P.N., *Thermophysical and thermodynamic properties of ionic liquids over an extended pressure range: [bmim][NTf2] and [hmim][NTf2]*. Journal of Chemical Thermodynamics, 2005. **37**(9): p. 888-899.

54. Gardas, R.L., Freire, M.G., Carvalho, P.J., Marrucho, I.M., Fonseca, I.M.A., Ferreira, A.G.M., and Coutinho, J.A.P., *P rho T measurements of imidazolium-based ionic liquids*. Journal of Chemical and Engineering Data, 2007. **52**: p. 1881-1888.

55. Valderrama, J.O., Sanga, W.W., and Lazzus, J.A., *Critical properties, normal boiling temperature, and acentric factor of another 200 ionic liquids*. Industrial & Engineering Chemistry Research, 2008. **47**(4): p. 1318-1330.

56. Valderrama, J.O. and Robles, P.A., *Critical properties, normal boiling temperatures, and acentric factors of fifty ionic liquids*. Industrial & Engineering Chemistry Research, 2007. **46**(4): p. 1338-1344.

57. Oliveira, M.B., Marrucho, I.M., Coutinho, J.A.P., and Queimada, A.J., *Surface tension of chain molecules through a combination of the gradient theory with the CPA EoS*. Fluid Phase Equilibria, 2008. **267**(1): p. 83-91.

APPENDIX

A. Critical Properties

Table A 1 Molecular weight and critical properties for CO_2, CCl_4 and CS_2 [51].

Compound	M_r (kg mol^{-1})	T_c (K)	P_c (MPa)	w
CO_2	0.04401	304.21	7.38	0.22362
CCl_4	0.15382	556.35	4.56	0.192552
CS_2	0.07614	552.00	7.90	0.110697

Table A 2 Molecular weight and critical properties of the $[C_n mim][NTf_2]$ family [55, 56].

Compound	M_r (kg mol^{-1})	T_c (K)	P_c (MPa)	w
$[C_2mim][NTf_2]$	0.39132	1244.9	3.26	0.1818
$[C_3mim][NTf_2]$	0.40534	1259.3	2.99	0.2573
$[C_4mim][NTf_2]$	0.41937	1265.0	2.76	0.2656
$[C_5mim][NTf_2]$	0.43338	1281.1	2.56	0.3442
$[C_6mim][NTf_2]$	0.44742	1287.3	2.39	0.3539
$[C_7mim][NTf_2]$	0.46145	1305.0	2.23	0.4349
$[C_8mim][NTf_2]$	0.47548	1311.9	2.10	0.4453

B. Vapour pressure and liquid density parameters correlation

Table B 1 Parameters used in the vapour pressure correlation for CO_2, CCl_4 and CS_2 [51].

Compound	A	B	C	D	E
CO_2	140.54	-4735	-21.268	4.0909×10^{-2}	1.0
CCl_4	78.44	-6128	-8.5766	6.8465×10^{-6}	2.0
CS_2	67.11	-4820	-7.5303	9.1695×10^{-3}	1.0

Table B 2 Parameters used in the liquid density correlation for CO_2, CCl_4 and CS_2 [51].

Compound	A	B	C	D
CO_2	2.768	0.262	304.21	0.291
CCl_4	0.998	0.274	556.35	0.287
CS_2	1.796	0.287	552.00	0.323

Table B 3 Parameters used in the vapour pressure correlation for the $[C_n mim][NTf_2]$ family.

Compound	A	-B (K)
$[C_2mim][NTf_2]$	27.12	-14286
$[C_3mim][NTf_2]$	24.68	-13300
$[C_4mim][NTf_2]$	26.98	-14235
$[C_5mim][NTf_2]$	27.50	-14473
$[C_6mim][NTf_2]$	28.85	-15192
$[C_7mim][NTf_2]$	29.15	-15318
$[C_8mim][NTf_2]$	29.58	-16409